Environ Monit Assess (2019) 191: 317
https://doi.org/10.1007/s10661-019-7430-3

The synergistic role of agricultural activities in groundwater quality in ultramafic environments: the case of the Psachna basin, central Euboea, Greece

Panagiotis Papazotos · Eleni Vasileiou · Maria Perraki

Received: 30 September 2018 / Accepted: 20 March 2019 / Published online: 30 April 2019

Abstract In the present study, we approach the geochemical processes affecting the hydrochemistry and resulting in elevated concentrations of hexavalent chromium (Cr^{6+}) in groundwater of the Psachna basin, central Euboea, Greece. Sixty-five groundwater samples and 16 topsoil (5–20 cm) samples were studied in order to examine groundwater and soil quality in relation to geogenic processes and anthropogenic activities. Specifically, the origin of Cr and Cr^{6+} in groundwater was investigated by co-evaluating (a) hydrochemical cross plots of major ions; (b) spatial distribution maps of Cl^-, Mg^{2+}, NO_3^-, and Cr^{6+}; (c) multivariate statistical analyses such as factor analysis (FA) and hierarchical cluster analysis (HCA) of groundwater geochemistry; (d) chemical analyses of soil samples; and (e) chemical analyses of fertilizers. The major factors that control the hydrochemistry of the study area are reverse ion exchange, dissolution of silicate minerals, and intense agricultural activities. According to FA, three factors explain 73.2% of the total variance of data, whereas according to HCA, the groundwater samples were classified into three groups indicating both geogenic (water–rock interaction) and anthropogenic (agricultural activities) impact. The high concentration of NO_3^-, up to 540 mg L^{-1}; the strong positive correlation between NO_3^- and Cr as well as between NO_3^- and other parameters such as SO_4^{2-} and Mg^{2+} in groundwater samples; and the very high content of P, up to 2444 mg kg^{-1}, in soil samples of the Psachna basin, imply the synergistic, although commonly neglected, role of the use of fertilizers in groundwater quality.

Keywords Euboea · Chromium · Multivariate statistical analysis · Fertilizers · Groundwater

P. Papazotos · E. Vasileiou · M. Perraki (✉)
School of Mining and Metallurgical Engineering, Division of Geo-sciences, National Technical University of Athens, 9 Heroon Polytechniou St., 15773 Zografou, Greece
e-mail: maria@metal.ntua.gr

Introduction

Geochemistry of ultramafic environments is strongly depicted on groundwater quality. Ultramafic rocks and serpentine soils and sediments exhibit high content in magnesium (Mg), iron (Fe), arsenic (As), cobalt (Co), chromium (Cr), manganese (Mn), and nickel (Ni) in relation to the Earth's crust composition (Oze et al. 2004; Rajapaksha et al. 2012; Kelepertzis et al. 2013; Kumarathilaka et al. 2014 and references therein). As a result, groundwater aquifers developed in ultramafic environments have been reported to exhibit elevated concentrations of major ions such as Mg^{2+}, bicarbonates (HCO_3^-), and trace elements such as Cr and As (Fantoni et al. 2002; Marques et al. 2008; Ryan et al. 2011; Margiotta et al. 2012; Kaitantzian et al. 2013; Tashakor et al. 2018). Differences in geochemical characteristics prevailing, i.e., pH, Eh, dissolved oxygen, organic matter, and degree of weathering, control the mobility and total concentration of these elements in groundwater.

Cr has attracted much attention among other potentially harmful trace elements (PHTE). The most common species of Cr in nature is the trivalent one (Cr^{3+}),

which is an essential nutrient in humans, animals, and plants. However, exposure to high levels via inhalation, ingestion, or dermal contact may cause adverse health effects (Wilbur et al. 2000; Saha et al. 2011; Zhitkovich 2011). Hexavalent chromium (Cr^{6+}) has been shown in experiments in rats to be a carcinogen via the inhalation route, although the limited data available do not show evidence for carcinogenicity via the oral route. In epidemiological studies, an association has been found between exposure to Cr^{6+} by the inhalation route and lung cancer (WHO 2011). Difficulties exist in distinguishing between the effects caused by Cr^{6+} and those caused by Cr^{3+} since Cr^{6+} is rapidly reduced to Cr^{3+} after penetration of biological membranes and in the gastric environment (Petrilli et al. 1986). The reduction of Cr^{6+} to Cr^{3+} inside of cells may be an important mechanism for the toxicity of Cr compounds, whereas the reduction of Cr^{6+} to Cr^{3+} outside of cells is a major mechanism of protection. The United States Environmental Protection Agency (USEPA) has included Cr in a list of 126 priority pollutants (USEPA 2014). However, the complexity of factors to be considered when evaluating the toxicity of Cr compounds as well as analytical difficulties in precisely analyzing them has led the World Health Organization (WHO) and European Union to set a maximum guideline value of 50 μg L^{-1} in drinking water only for Cr (WHO 2011; Council Directive 98/83/EC), whereas no value has been set yet for Cr^{6+}. Similarly, the USEPA (2011) has set the maximum acceptable concentration for Cr at 100 μg L^{-1} in most states of the USA, whereas the Dutch intervention value for Cr has been set at 30 μg L^{-1} (VROM 2000).

The role of geogenic input of Cr and other PHTE in soils and groundwater in ultramafic environments as well as of natural oxidizing factors such as manganese oxides in the oxidation of Cr^{3+} to Cr^{6+} has been increasingly highlighted in the last decade. Geogenic Cr may be derived by natural processes such as weathering of Cr-bearing ultramafic complexes. Common minerals that host Cr are spinels such as chromite and magnetite; silicate primary minerals such as pyroxene and olivine; silicate secondary minerals such as amphibole, serpentine, chlorite, talc, and clays; and Fe-hydroxides, mainly goethite (e.g., Fantoni et al. 2002; Oze et al. 2004; Morrison et al. 2009; Economou-Eliopoulos et al. 2011). The crystal lattice of the most abundant rock-forming Cr-bearing minerals hosts Cr^{3+}, except for very rare minerals such as crocoite ($PbCrO_4$) in which Cr is hexavalent. Whereas Cr^{3+} is mobilized in acid conditions (Richard and Bourg 1991; Kotaś and Stasicka 2000), Cr^{6+} exhibits high mobility in alkaline conditions characterizing ultramafic environments (Kotaś and Stasicka 2000); therefore, relatively elevated concentrations of Cr and Cr^{6+} are expected in groundwater aquifers developed in ultramafic environments.

Manganese oxides in the form of birnessite/δ-MnO_2 (Fendorf and Zasoski 1992; Fendorf et al. 1992; Oze et al. 2007; Rajapaksha et al. 2013), pyrolousite/β-MnO_2 (Eary and Rai 1987), asbolane-type/$(Ni,Co)_{1-x}(Mn^{IV}O_2)_{2-y}(OH)_{2-2x+2y}{\cdot}nH_2O$, lithiophorite-type/$(Al,Li)Mn^{iv}O_2(OH)_2$ (Fandeur et al. 2009), and cryptomelane/$K(Mn^{iv}_7Mn^{iii})O_{16}$ (Feng et al. 2007) in rocks and soils have been reported to act as natural oxidizing agents under favorable pH and redox conditions (Kožuh et al. 2000; Fantoni et al. 2002; Kazakis et al. 2015).

Water–soil–rock interaction has resulted in elevated Cr^{6+} concentrations in many areas in Greece (Megremi 2010a, 2010b; Economou-Eliopoulos et al. 2011; Economou-Eliopoulos et al. 2012; Moraetis et al. 2012; Tziritis et al. 2012; Kaitantzian et al. 2013; Dermatas et al. 2015; Kaprara et al. 2015; Megremi et al. 2019) and in the rest of the world such as the USA (Oze et al. 2004; Gonzalez et al. 2005; Morrison et al. 2009), Italy (Fantoni et al. 2002), Brazil (Bourotte et al. 2009; Bertolo et al. 2011), Mexico (Robles-Camacho and Armienta 2000), New Caledonia (Becquer et al. 2003), and Zimbabwe (Cooper 2002). In the aforementioned areas, Cr^{6+} concentration exhibits a wide range from less than 2 up to 130 μg L^{-1} (Bertolo et al. 2011); conditions such as the aquifer media, the depth of the aquifer, and seasonal climate variations seem to define the maximum concentration even in similar geological environments.

Anthropogenic Cr has been related to industrial wastes from metallurgy, refractory, chemical manufacturing, etc. (Jacobs and Testa 2004; Rakhunde et al. 2012), and it can be either Cr^{3+} or Cr^{6+} depending on the industrial process.

Agricultural activities have been related to mobilization of PHTE from cultivated soils to groundwater (Becquer et al. 2003; Izbicki et al. 2008; Mills et al. 2011; Remoundaki et al. 2016; Hausladen et al. 2018). Phosphorous (P)-bearing fertilizers are the main source of PHTE between the three major fertilizer types, i.e., nitrogen (N)-bearing, phosphorous (P)-bearing, and potassium (K)-bearing fertilizers (Sager 1997; Nicholson

et al. 2003). The majority of P-bearing fertilizers are produced from phosphate rocks which are a possible source of PHTE since they are enriched in trace elements such as As, Cd, Cr, Cu, Ni, Pb, and Zn (Mortvedt 1996; Faridullah et al. 2017). Modaihsh et al. (2004) and Molina et al. (2009) showed that PHTE concentrations in fertilizers varied widely with the P-bearing fertilizers having the highest Cr content. Furthermore, agricultural and other anthropogenic activities such as unsewered sanitations, livestock wastes, and sewage effluents result in high concentration of NO_3^- in groundwater (McLay et al. 2001) compared to areas relatively unaffected by human activities in which NO_3^- concentrations are less than 10 mg L^{-1} (Panno et al. 2006). Mills et al. (2011) and Mills and Goldhaber (2012) related the use of N-bearing fertilizers to elevated concentration of Cr^{6+} in surficial layers of soils. A proposed possible mechanism is that the process of nitrification (oxidation of NH_4^+ to NO_3^-) results in the production of H^+ and soil acidification, favoring the increased dissolution of Cr^{3+} which is subsequently oxidized into Cr^{6+} by natural and/or anthropogenic factors.

In the Psachna basin, central Euboea, Greece, which is an ultramafic-dominated environment, elevated Cr concentration in groundwater has been reported since 2010 (Megremi 2010b). To date, an increasing number of studies have tried to approach the geochemical processes that control the mobility and bioavailability of Cr and Cr^{6+}, mainly placing emphasis on the geological environment (Megremi 2010a; Economou-Eliopoulos et al. 2013, 2014, 2017; Voutsis et al. 2015). Besides, Vasileiou et al. (2014a, b), Remoundaki et al. (2016), and Megremi et al. (2019) highlighted the strong positive correlation between NO_3^- and Cr^{6+} in groundwater of the Psachna basin. However, the exact mechanism of relating NO_3^- to Cr^{6+} has yet to be defined.

The complexity of the oxidizing factors of Cr^{3+}, the synergistic role of anthropogenic activities in elevated Cr and Cr^{6+} concentration in groundwater in ultramafic environments along with the usually neglected effect of fertilizers, the debatable background threshold for geogenic Cr, and the lack of a reliable and widely accepted quantitative method for distinguishing and quantifying geogenic and anthropogenic Cr input constitute a challenging field of research for further investigation.

In this study, we aim to elucidate the major factors affecting the hydrochemistry and resulting in elevated concentrations of Cr and Cr^{6+} in groundwater of the Psachna basin, central Euboea, Greece. In addition to geochemical processes controlling the geogenic input, we study the synergistic role of agricultural activities in groundwater quality in an ultramafic environment as that characterizing the Psachna basin, focusing on the use of N-bearing and P-bearing fertilizers. Specifically, the origin of Cr and Cr^{6+} in groundwater was investigated by co-evaluating (a) hydrochemical cross plots of major ions; (b) spatial distribution maps of Cl^-, Mg^{2+}, NO_3^-, and Cr^{6+}; (c) factor analysis (FA) and hierarchical cluster analysis (HCA) of groundwater geochemistry; (d) chemical analyses of soil samples; and (e) chemical analyses of fertilizers. Elucidating the role of the use of fertilizers in already geogenically degraded soils will contribute to define the best practices available in improving the environmental sustainability of water management and agriculture in ultramafic-dominated areas.

Study area

Geological and hydrogeological setting

The Psachna basin is located in the central part of Euboea island and lies between the latitudes 38 32′00 and 38 36′28′ N and the longitudes 23 32′00 and 23 43′ 00′ E; altitudes range from 0–15 m in the coastline, to 20 m in the Psachna town and up to 200 m in the northern part of the basin. The dominant geological formations apart from Quaternary and Neogene sediments (alluvial, marls, conglomerates, sandstones) located mainly in lowland areas are Cretaceous carbonate formations (limestones, dolomites), ultramafic/mafic rocks (serpentinites, peridotites, diabases), and Fe–Ni ore deposits (Katsikatsos et al. 1980, 1981). Figure 1 presents a simplified geological map of the study area with the sampling sites. The main aquifer systems that are developed in central Euboea are (a) the Dirfys karstic system, (b) a shallow alluvial aquifer, (c) a Neogene aquifer, and (d) a fractured aquifer in ultramafic rocks. The geological formations in central Euboea in terms of their permeability are characterized as (a) permeable (limestones–dolomites–alluvial deposits–conglomerates–sandstones), (b) impermeable (clays, marls, ultramafic rocks), and (c) semipermeable (fractured ultramafic rocks) (Tsioumas and Zorapas 2004; Dandolos and Zorapas 2010). The main aquifer system studied herein is the alluvial one, which expands in a total area of 21 km^2, with the lowest part to be coastal. It is

developed within Quaternary sediments and consists of the products of the erosion of ultramafic rocks and limestones. The unsaturated zone (UZ) in the study area is mainly unconfined but locally appears confined depending on the presence of marls and clays (Voutsis et al. 2015). The natural recharge of the groundwater in the Psachna basin is achieved via the precipitations, the infiltrations of the surface runoff (torrents) and the lateral inflows from groundwater systems developed in the carbonate (part of the Dirfys karstic system), and fractured ultramafic rocks at the north part of the basin (Tsioumas and Zorapas 2004; Dandolos and Zorapas 2010). The hydraulic conductivity of the alluvial aquifer was estimated about 2×10^{-4} m s^{-1} (Gyftoulas et al. 2017). The thickness of the UZ in the study area ranges from 0.8 m in the coastal zone up to 6.8 m in the central part of the basin (Gyftoulas et al. 2017). Natural springs flow out in the contact of limestones and ultramafic rocks in the central–northern part and in the contact of limestones and Quaternary sediments in the coastal area.

Land uses

Agriculture is the major land use in the Psachna basin. The main products obtained from agricultural activities, according to recent data provided by the Greek Payment and Control Agency for Guidance and Guarantee Community Aid (OPEKEPE 2014), are cereals and horticultural plants, whereas minor products are olive groves and legumes. Carrots, potatoes, cabbages, lettuces, and broccoli crops were also observed during fieldwork.

Methods

Groundwater sampling and determinations

Two datasets are processed in the present study. The first dataset includes 41 samples and corresponds to four different seasonal samplings representative of dry and wet periods and was conducted during November 2014, December 2016, June 2017, and November 2017. All samples were collected at least 1 week after the last rainfall had taken place to avoid any direct impact effect of rainfall to groundwater. Dataset 1 includes samples from 38 irrigation drills in the alluvial aquifer and three springs. Emphasis was placed on 22 physical and chemical parameters (electrical conductivity—EC, pH, total dissolved solids—TDS, Ca^{2+}, Mg^{2+}, K^{+}, Na^{+}, HCO_3^{-}, NO_3^{-}, Cl^{-}, SO_4^{2-}, As, Cd, Co, Cr, Cr^{6+}, Cu, Fe, Ni, P, Pb, and Zn) of the groundwater samples. Each sample of 1000 mL collected from each sampling site was divided into three subsamples: one to determine major anions and cations: one to determine trace elements after filtering through a 0.45-μm filter and acidifying with 1 M HNO_3, and one to determine Cr^{6+} by ion exchange using IC-All tech cartridges (Ball and McCleskey 2003). The EC and pH for the first dataset were measured in situ immediately after samples were collected according to YSI Professional Digital Sampling System (ProDSS). Dissolved major cations (Ca^{2+}, Mg^{2+}, Na^{+}, and K^{+}) were analyzed in a nonacidified sample by atomic absorption spectrometry; NO_3^{-} was analyzed by spectrophotometry, Cl^{-} and HCO_3^{-} were analyzed by titrimetry, and SO_4^{2-} was analyzed by turbidimetric determination. The analyses of trace elements (As, Cd, Co, Cr, Cu, Fe, Ni, Pb, P, and Zn) were performed at Analytical Laboratories of Bureau Veritas Commodities Canada Ltd., by means of inductively coupled plasma mass spectrometry (ICP-MS), whereas Cr^{6+} was determined by ICP-MS Agilent Technologies 7700 series in the School of Mining and Metallurgical Engineering of National Technical University of Athens, Greece. TDS were calculated directly from the summation of the major ions. The laboratory of Bureau Veritas Commodities Canada Ltd. is accredited to the ISO/IEC 17025:2005 standard, which includes both quality assurance and quality control protocols. The second dataset includes 24 samples out of a total of 30 samples and corresponds to the study of Remoundaki et al. (2016), the sampling of which was held during November 2012, April 2013, and April 2015. Six samples were excluded from processing due to their sparse spatial distribution outside the boundaries of the study area. This dataset includes 18 samples from irrigation drills in the alluvial aquifer, five samples from springs, and one sample from a mining pit (Makrimalli village). The spatial distribution of the groundwater samples of the two datasets is presented in Fig. 1.

Soil sampling and chemical analysis

Sixteen composite topsoil (5–20 cm) samples were collected during November 2017 from the sites presented in Fig. 1. At each sampling site, one sample was collected by compositing five different subsamples from the corners and the center of a total 25 m^2 square, in sealable plastic bags using a plastic spatula. Since it has been strongly suggested that chromite ($FeCr_2O_4$) is not completely

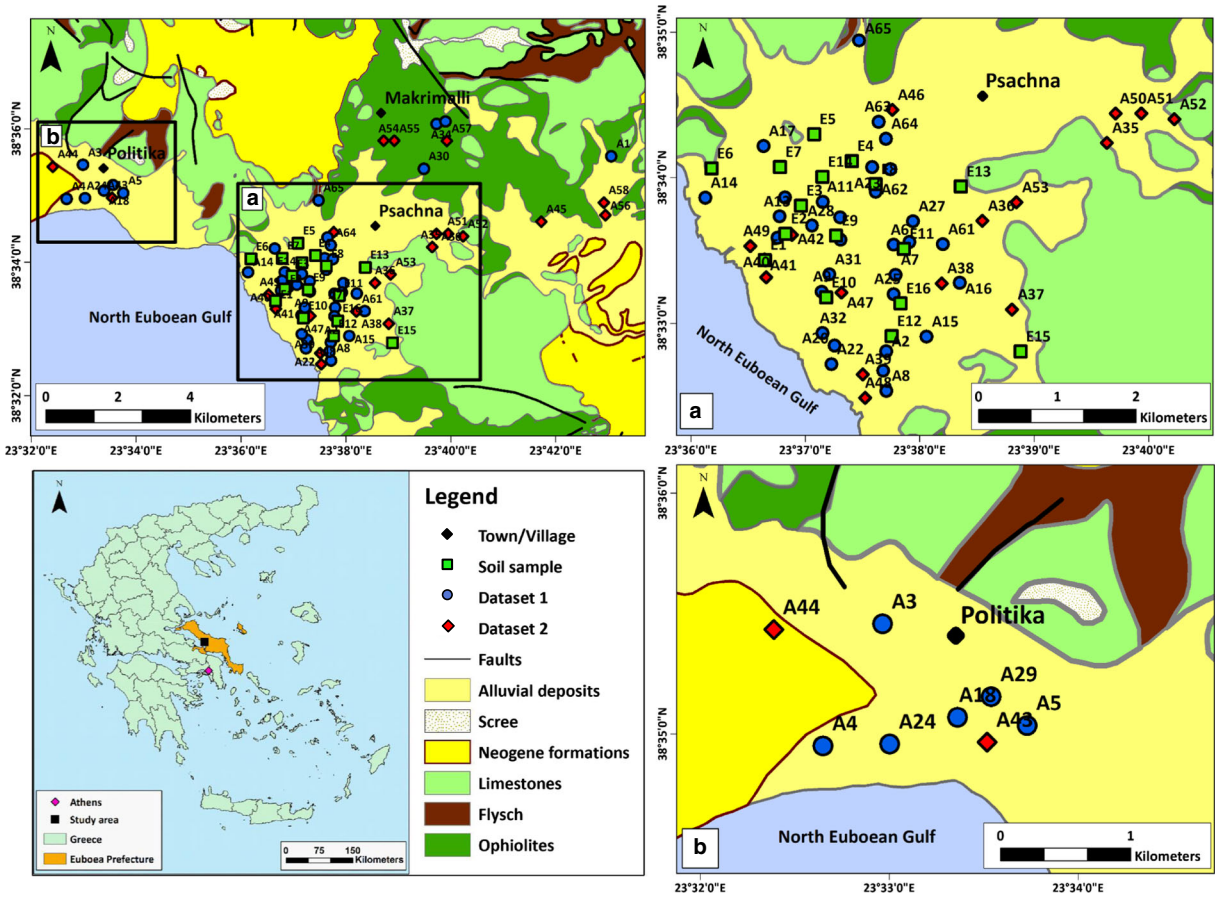

Fig. 1 A simplified geological map of the study area (after Katsikatsos et al. 1981) and sampling sites. Enlarged images of the Psachna and the Politika areas are given in **a** and **b**, respectively

dissolved by four acid digestion (HNO_3, HCl, HF, $HClO_4$), a case that should be taken into consideration in geochemical studies carried out in ultramafic environments (Morrison et al. 2009), chemical analyses of pulp soil samples (major and trace elements) were determined by lithium borate fusion and aqua regia methods followed by X-ray fluorescence (XRF) for major elements (SiO_2, Al_2O_3, Fe_2O_3, MgO, CaO, Na_2O, K_2O, TiO_2, P_2O_5, MnO, and Cr_2O_3) and ICP-MS for trace elements at Analytical Laboratories of Bureau Veritas Commodities Canada Ltd.

Fertilizer analyses

Chemical analyses of P-bearing fertilizers (P1, P2, and P3) of N–P–K composition 0–46–0, 17.5–44–0, and 28–28–0, respectively, obtained from local fertilizer markets, were analyzed for trace elements at Analytical Laboratories of Bureau Veritas Commodities Canada Ltd., by ICP-MS.

Data processing

Spatial distribution maps were generated using ArcGIS v10.3. Statistical analysis of groundwater and soil data was carried out with IBM SPSS version 22 software.

Data were evaluated by applying the Pearson's correlation coefficient, the chloro-alkaline indices, and two multivariate statistical techniques, the FA and the HCA. The Pearson's correlation coefficient (r) measures the statistical association between pairs of different continuous parameters. The r values can take on any value in the range between −1 and 1. The direction of the relationship is indicated by the sign of the coefficient; a positive sign (+) indicates a positive relationship and a negative sign (−) sign indicates a negative relationship between the two examined parameters.

$$r_{xy} = \frac{\sum_{i=1}^{n}\left(x_i-\bar{x}\right)\left(y_i-\bar{y}\right)}{\sqrt{\sum_{i=1}^{n}\left(x_i-\bar{x}\right)^2 \sum_{i=1}^{n}\left(y_i-\bar{y}\right)^2}}$$

where, r_{xy} = correlation coefficient value between parameters x and y, n = sample size, x_i = individual value of parameter x, $\bar{x}$ = mean value of parameter x, y_i = individual value of parameter y, and $\bar{y}$ = mean value of parameter y. Correlation coefficient is classified as very strong, strong, moderate, weak, and very weak corresponding to absolute values of 0.80–1, 0.60–0.79, 0.40–0.59, 0.20–0.39, and less than 0.20, respectively (Evans 1996).

Chloro-alkaline indices (CAI1 and CAI2) suggested by Schoeller (1977) were calculated according to the following equations:

$$\mathrm{CAI1} = \mathrm{Cl}^- - \left(\mathrm{Na}^+ + \mathrm{K}^+\right)/\mathrm{Cl}^-$$

$$\mathrm{CAI2} = \mathrm{Cl}^- - \left(\mathrm{Na}^+ + \mathrm{K}^+\right)/\mathrm{SO_4}^{2-} + \mathrm{HCO_3}^- + \mathrm{NO_3}^-, \left(\text{All values are expressed in meq } \mathrm{L}^{-1}\right)$$

In the case of an exchange of Ca^{2+} and/or Mg^{2+} in groundwater with Na^+ and/or K^+ in aquifer media, both the abovementioned indices are negative, whereas in the case of a reverse ion exchange, they are both positive (Schoeller 1977). So far, chloro-alkaline indices have been extensively used to identify the ion exchange between the groundwater and the aquifer media (Kumar et al. 2007; Aghazadeh and Mogaddam 2011; Singh et al. 2013, 2014; Toumi et al. 2015).

FA is a statistical procedure to identify interrelationships among a large number of parameters and to investigate the way in which the associations between the examined parameters are affected. A new set of noncorrelated parameters were created in order to reduce the dimension of the data with the method of principal component analysis (PCA). The technique of Varimax rotation using the Kaiser procedure (Kaiser 1958) and the scree plot method (Cattell 1966) was used to separate and identify the distributions associated with individual components. The factors with eigenvalues higher than 1 are significant according to Kaiser criterion and the rest are eliminated. Factor loadings are classified into three groups in order to determine the relations between the parameters. Three classes with absolute values > 0.75, 0.5–0.75, and 0.5–0.3 are distinguished into strong, moderate, and weak, respectively (Liu et al. 2003). The Kaiser–Meyer–Olkin (KMO) and the Bartlett's tests were used to evaluate the FA method. Supplementary to FA, HCA constitutes a further approach for the multivariate statistical analysis in order to approach the factors which affect groundwater chemistry (e.g., Voutsis et al. 2015; Tziritis et al. 2016). The HCA is used to classify groundwater samples into clusters using as linkage the Ward's method (Ward 1963) and as similarity measure the squared Euclidian distances which is the most common measure of distance in hydrochemical studies; samples are distinguished by high homogeneity and heterogeneity depending on whether they belong to the same cluster or not.

Results

Groundwater chemistry

Sampling site coordinates and physical and chemical parameters of the groundwater samples of the Psachna basin studied herein are shown in Table 1. Descriptive statistics of groundwater samples are presented in Table 2; for comparison, the guideline values for drinking water of WHO (2011) are also given. The value ranges of the two datasets are provided separately in order to highlight the fluctuation of the studied parameters.

The pH value ranges from 6.8 to 8.27 (mean 7.5) and the EC from 334 to 5129 μS cm^{-1} (mean 1234.32 μS cm^{-1}). The major ions, as well as Cr and Cr^{6+}, present high variation in the Psachna basin. Cr concentration ranges from 4 to 161.5 μg L^{-1} (mean 57.15 μg L^{-1}) and Cr^{6+} from 2 to 146 μg L^{-1} (mean 49.84 μg L^{-1}). The concentration of NO_3^- ranges from 4.7 to 540 mg L^{-1} (mean 124.60 mg L^{-1}).

As mentioned above, in dataset 1, concentrations of Cd, Co, Cu, Fe, Mn, Ni, P, Pb, and Zn were additionally analyzed (Table 2); they are all below the guideline values for drinking water of WHO (2011).

Water type

The chemistry of groundwater samples indicates the hydrochemical nature of groundwater with respect to aquifer. A trilinear diagram (Fig. 2; Piper 1944) was used to determine the main groundwater types in the study area. The cationic triangle is dominated by the presence of Ca^{2+}

Table 1 Location, sample type, and physical and chemical parameters for 65 groundwater samples ($N = 65$) of the Psachna basin

ID	Dataset	Type	X	Y	pH –	EC μS cm^{-1}	TDS mg L^{-1}	Ca^{2+} mg L^{-1}	Mg^{2+} mg L^{-1}	Na^{+} mg L^{-1}	K^{+} mg L^{-1}	HCO_3^{-} mg L^{-1}	SO_4^{2-} mg L^{-1}	Cl^{-} mg L^{-1}	NO_3^{-} mg L^{-1}	Cr μg L^{-1}	Cr^{6+} μg L^{-1}
A1	1	Spring	23° 43′ 2.521″ E	38° 35′ 37.466″ N	7.81	1062	782.50	36.4	116	17.2	1.3	525	10	30	56.6	52.2	48.33
A2	1	Irrigation drill	23° 37′ 42.314″ E	38° 32′ 48.862″ N	7.85	969	557.44	70.6	52.6	31.6	2.94	166	30	119	84.7	35.1	35.1
A3	1	Irrigation drill	23° 32′ 57.559″ E	38° 35′ 27.680″ N	7.87	701	448.95	77	32.2	15.1	2.35	251	10	39	32.3	4	4
A4	1	Irrigation drill	23° 32′ 38.780″ E	38° 34′ 57.198″ N	7.72	943	659.50	86.6	51.1	45.4	1.3	326	25	98	26.1	16.9	16.9
A5	1	Irrigation drill	23° 33′ 31.277″ E	38° 35′ 7.038″ N	7.6	1104	739.03	89	69	47.5	1.23	322	86	81	43.3	36.5	30.92
A6	1	Irrigation drill	23° 37′ 54.071″ E	38° 33′ 34.186″ N	7.22	987	762.80	102	64.9	31.9	2.1	327	87	51	96.9	57.7	47.3
A7	1	Irrigation drill	23° 37′ 46.065″ E	38° 33′ 12.453″ N	7.55	1069	830.80	99.3	66.8	30.2	1.5	265	117	62	189	79.8	68.61
A8	1	Irrigation drill	23° 37′ 40.831″ E	38° 32′ 40.942″ N	7.87	783	566.63	64.4	49.3	23.9	2.93	248	16	98	64.1	81.3	72.16
A9	1	Irrigation drill	23° 37′ 10.815″ E	38° 33′ 16.520″ N	7.52	1339	1012.82	103	88.5	40.8	1.52	318	150	87	224	85.7	74.44
A10	1	Irrigation drill	23° 37′ 18.144″ E	38° 33′ 34.704″ N	7.51	960	764.89	75.9	66.7	35.3	0.99	326	78	48	134	68.6	62.17
A11	1	Irrigation drill	23° 37′ 8.640″ E	38° 33′ 50.343″ N	7.61	1184	936.54	95.6	86.3	36.3	1.34	354	104	59	200	121.1	111.5
A12	1	Irrigation drill	23° 36′ 48.952″ E	38° 33′ 52.074″ N	7.46	1166	950.86	109	72.1	24.9	0.86	314	119	69	242	120.6	89.74
A13	1	Irrigation drill	23° 36′ 52.574″ E	38° 33′ 39.805″ N	7.4	1710	1357.99	131	102	72.6	4.39	322	236	140	350	99.3	89.23
A14	1	Irrigation drill	23° 36′ 39.596″ E	38° 33′ 39.722″ N	7.71	5129	3237.32	268	208	604	4.82	322	285	1460	85.5	83.89	83.89
A15	1	Irrigation drill	23° 38′ 3.312″ E	38° 32′ 54.921″ N	7.8	1397	894.42	113	83.5	43.4	2.52	265	109	154	124	64.6	56.86
A16	1	Irrigation drill	23° 38′ 20.710″ E	38° 33′ 17.303″ N	7.61	941	738.18	85.6	52.8	44.3	1.48	324	65	59	106	53.5	45.63
A17	1	Irrigation drill	23° 36′ 37.399″ E	38° 34′ 13.217″ N	7.56	2481	1743.7	127	175	99.5	26.2	246	161	369	540	161.5	131.1
A18	1	Irrigation drill	23° 33′ 31.323″ E	38° 35′ 7.085″ N	7.38	1077	830.08	98.5	63.2	44.1	1.18	387	98	94	44.1	41.1	38.94
A19	1	Spring	23° 39′ 49.566″ E	38° 36′ 7.344″ N	7.83	789	696.33	99.3	46	17.4	0.63	383	51	30	69	35.1	31.88
A20	1	Irrigation drill	23° 37′ 4.580″ E	38° 32′ 48.573″ N	7.84	842	555.2	59.2	54.6	27.4	5.4	199	24	133	52.6	88.8	80.65
A21	1	Irrigation drill	23° 36′ 44.971″ E	38° 33′ 35.510″ N	7.79	1160	916.64	85.2	86	62.9	2.54	303	128	90	159	89.1	73
A22	1	Irrigation drill	23° 37′ 14.419″ E	38° 32′ 45.312″ N	7.64	921	617.11	71.5	57.7	31.3	3.71	239	27	144	42.9	65.3	55.12
A23	1	Irrigation drill	23° 37′ 34.551″ E	38° 34′ 4.819″ N	7.95	865	672.2	75	65.8	30.8	1.1	312	60	37	90.5	64.8	57.94
A24	1	Irrigation drill	23° 33′ 0.004″ E	38° 34′ 57.764″ N	8.27	624	520.97	67.5	38.7	14.5	0.57	339	18	27	15.7	78.3	74.79
A25	1				7.46	1177	829.28	104	66.8	32.9	1.58	268	117	66	173	75	62.37

Table 1 (continued)

ID	Dataset	Type	*X*	*Y*	pH –	EC µS cm^{-1}	TDS mg L^{-1}	Ca^{2+} mg L^{-1}	Mg^{2+} mg L^{-1}	Na^{+} mg L^{-1}	K^{+} mg L^{-1}	HCO_3^{-} mg L^{-1}	SO_4^{2-} mg L^{-1}	Cl^{-} mg L^{-1}	NO_3^{-} mg L^{-1}	Cr µg L^{-1}	Cr^{6+} µg L^{-1}
		Irrigation drill	23° 37′ 46.075″ E	38° 33′ 12.471″ N													
A26	1	Irrigation drill	23° 37′ 40.784″ E	38° 32′ 40.887″ N	7.68	857	559.75	64.4	53	26.6	3.35	249	10	101	52.4	72.9	58.73
A27	1	Irrigation drill	23° 37′ 54.112″ E	38° 33′ 34.104″ N	7.39	980	728.07	94.2	61.3	32	1.17	386	70	44	39.4	28	21.03
A28	1	Irrigation drill	23° 37′ 17.856″ E	38° 33′ 43.981″ N	7.56	1465	954.94	111	94.6	48.5	2.84	366	185	71	76	134.4	101
A29	1	Irrigation drill	23° 33′ 31.364″ E	38° 35′ 7.118″ N	7.21	1654	1232.46	131	109	72.6	1.76	591	159	135	33.1	12.6	10.56
A30	1	Spring	23° 39′ 27.823″ E	38° 35′ 25.701″ N	8.05	334	197.62	4.48	37.7	9.3	2.14	129	10	15	5	10.4	10.29
A31	1	Irrigation drill	23° 37′ 12.402″ E	38° 33′ 20.442″ N	7.34	1339	986.36	108	85.9	37.2	1.26	362	142	66	184	84.4	66.86
A32	1	Irrigation drill	23° 37′ 8.811″ E	38° 32′ 56.260″ N	7.4	1679	1187.55	133	106	54.5	2.05	289	310	133	160	45.2	35.05
A33	1	Irrigation drill	23° 37′ 3.081″ E	38° 33′ 40.624″ N	7.53	1436	1019.95	127	76.5	57.8	7.65	286	122	83	260	93.3	73.08
A34	1	Irrigation drill	23° 39′ 52.284″ E	38° 36′ 8.165″ N	7.67	996	733.93	63.2	82.7	30.7	3.33	394	39	43	78	71.2	59.67
A35	2	Irrigation drill	23° 39′ 37.622″ E	38° 34′ 15.068″ N	7.27	800	524.66	77.72	47.33	20.13	6.07	270.84	10.26	36.48	55.84	24.43	21.64
A36	2	Irrigation drill	23° 38′ 32.488″ E	38° 33′ 42.756″ N	7.31	887	655.79	91.25	55.06	23.71	1.1	345.26	13.24	39.71	86.45	57.09	52.84
A37	2	Irrigation drill	23° 38′ 48.244″ E	38° 33′ 6.240″ N	7.01	948	528.95	129.85	31.55	35.15	2.29	211.06	10.33	57.27	51.45	15.98	12.76
A38	2	Irrigation drill	23° 38′ 11.255″ E	38° 33′ 16.930″ N	7.27	1265	889.51	115.68	85.17	38.69	2.82	355.02	29.28	79.02	183.83	73.52	69.81
A39	2	Irrigation drill	23° 37′ 38.262″ E	38° 32′ 41.301″ N	7.44	981	639.53	67.66	64.49	38.54	4.25	281.82	5.33	145.2	32.25	63.51	63.43
A40	2	Irrigation drill	23° 36′ 42.399″ E	38° 33′ 21.738″ N	7.15	1522	948.55	114.24	120.21	51.39	1.73	367.22	76	110.79	106.98	45.45	41.1
A41	2	Irrigation drill	23° 36′ 38.200″ E	38° 33′ 26.526″ N	7.39	1739	1093.83	132.09	141.74	59.31	1.48	325.72	98.02	159.25	176.23	48.87	38.91
A42	2	Irrigation drill	23° 36′ 49.291″ E	38° 33′ 38.567″ N	7.23	2370	1473.3	197.58	155.97	92.5	5.28	280.6	89.53	199.72	452.12	92.22	88.68
A43	2	Irrigation drill	23° 33′ 31.407″ E	38° 35′ 6.956″ N	7.02	1204	784.11	112.41	75.58	50.25	1.57	353.8	32.24	112.25	46	34.9	34.27
A44	2	Irrigation drill	23° 32′ 22.960″ E	38° 35′ 26.126″ N	7.04	910	609.31	105.53	30.24	47.15	2.43	297.68	6.72	93.46	26.09	6.4	5
A45	2	Irrigation drill	23° 41′ 42.492″ E	38° 34′ 38.479″ N	7.19	1529	1025.77	113.07	123.53	34.41	2.35	309.88	28.71	72.18	341.64	69.48	63.58
A46	2	Irrigation drill	23° 37′ 44.983″ E	38° 34′ 28.320″ N	7.45	1855	1312.13	84.5	147.99	33.2	1.6	484.34	98	75	387.5	146	146
A47	2	Irrigation drill	23° 37′ 12.920″ E	38° 33′ 16.193″ N	7.46	1875	1430.35	82.5	159.89	55.4	2.6	387.96	315	103	324	68	66
A48	2	Spring	23° 37′ 31.382″ E	38° 32′ 29.632″ N	7.55	1810	1295.4	96.12	50.79	186.8	10.8	481.9	120	294	55	36	33
A49	2				7.56	1599	1136.8	67.28	61.72	168.8	11.6	390.4	130	191	116	68	63

Table 1 (continued)

ID	Dataset	Type	*X*	*Y*	pH –	EC µS cm^{-1}	TDS mg L^{-1}	Ca^{2+} mg L^{-1}	Mg^{2+} mg L^{-1}	Na^{+} mg L^{-1}	K^{+} mg L^{-1}	HCO_3^{-} mg L^{-1}	SO_4^{2-} mg L^{-1}	Cl^{-} mg L^{-1}	NO_3^{-} mg L^{-1}	Cr µg L^{-1}	Cr^{6+} µg L^{-1}
		Irrigation drill	23° 36′ 37.271″ E	38° 33′ 30.092″ N													
A50	2	Irrigation drill	23° 39′ 42.235″ E	38° 34′ 27.183″ N	7.46	634	474.25	88.11	14.82	17.3	7.1	257.42	29	26	34.5	32	29
A51	2	Irrigation drill	23° 39′ 55.666″ E	38° 34′ 27.221″ N	7.36	695	522.13	89.31	21.14	22.1	1	273.28	44	26	45.3	34	31
A52	2	Irrigation drill	23° 40′ 12.993″ E	38° 34′ 24.935″ N	7.33	1210	931.66	113.34	73.39	28.3	1.5	478.24	94	39	103.9	85	84
A53	2	Irrigation drill	23° 38′ 50.342″ E	38° 33′ 50.434″ N	7.43	1687	1273.98	145.77	95.74	43.4	1.3	314.76	210	59	404	62	62
A54	2	Spring	23° 38′ 53.888″ E	38° 35′ 50.679″ N	7.09	881	1269.62	121.75	36.94	21.6	0.7	923.54	71	27.8	66.3	28	26
A55	2	Spring	23° 38′ 53.888″ E	38° 35′ 50.646″ N	7.22	886	734.63	96.12	44.71	24.2	1.6	451.4	47	25.8	43.8	48	40
A56	2	Pit lake	23° 42′ 53.862″ E	38° 34′ 50.663″ N	7.7	500	591.54	86.5	7.78	17.5	2.4	406.26	15	48.7	7.4	4	2
A57	2	Spring	23° 39′ 53.874″ E	38° 35′ 50.660″ N	6.8	818	923.17	147.38	15.55	21.6	0.7	691.74	15	22.7	8.5	25	20
A58	2	Spring	23° 42′ 53.862″ E	38° 34′ 50.663″ N	7.6	1098	1212.14	51.26	104.98	19.9	3.6	976	12	8	36.4	44	37
A59	1	Irrigation drill	23° 37′ 44.092″ E	38° 34′ 3.962″ N	7.52	937	804.3	72.7	38.4	35.8	1.6	488	70	32	65.8	22	14
A60	1	Irrigation drill	23° 37′ 54.322″ E	38° 33′ 33.962″ N	7.47	962	811.2	45.4	66.8	33.2	1.3	494	57	40	73.5	15	10
A61	1	Irrigation drill	23° 38′ 11.791″ E	38° 33′ 33.063″ N	7.45	1346	987.9	68.2	80.7	47.1	2.7	427	127.5	98	136.7	40	25
A62	1	Irrigation drill	23° 37′ 36.492″ E	38° 33′ 54.562″ N	7.46	1547	997.8	73.4	101.6	46.6	1.7	366	185	80	143.5	34	21
A63	1	Irrigation drill	23° 37′ 37.791″ E	38° 34′ 23.462″ N	7.63	1195	794.8	47.9	88.7	35.2	0.9	366	92.5	42	121.6	21	17
A64	1	Irrigation drill	23° 37′ 41.691″ E	38° 34′ 16.462″ N	7.58	1139	965.7	51.7	79.2	35.7	3.3	500	140	44	111.8	27	21
A65	1	Irrigation drill	23° 37′ 27.491″ E	38° 34′ 56.863″ N	7.48	1282	923.4	57.4	51	14	16.5	476	140	47	121.5	32	22

Table 2 Descriptive statistical parameters of the analyzed groundwater samples in the Psachna basin ($N = 65$)

Parameter	Unit	Dataset 1 ($N = 41$)	Dataset 2 ($N = 24$) (Remoundaki et al. 2016)	All data ($N = 65$)			WHO guideline (2011)
		Range	Range	Mean	Min	Max	
pH	–	7.21–8.27	6.8–7.7	7.5	6.8	8.27	6.5–8.5
EC	μS cm^{-1}	334–5129	500–2370	1234.32	334	5129	2500
TDS	mg L^{-1}	197.62–3237.32	474.25–1473.3	904.45	197.62	3237.32	–
Ca^{2+}	mg L^{-1}	4.48–268	45.4–197.58	94.98	4.48	268	–
Mg^{2+}	mg L^{-1}	32.2–208	7.78–159.89	75.31	7.78	208	–
Na^{+}	mg L^{-1}	9.3–604	14–186.8	50.36	9.3	604	200
K^{+}	mg L^{-1}	0.57–26.2	0.7–16.5	3.2	0.57	26.2	12
HCO_3^{-}	mg L^{-1}	129–591	211.06–976	365.17	129	976	–
SO_4^{2-}	mg L^{-1}	8–310	5.33–315	87.23	5.33	315	250
Cl^{-}	mg L^{-1}	15–1460	8–294	104.14	8	1460	250
NO_3^{-}	mg L^{-1}	4.7–540	7.4–452.12	124.6	4.7	540	50
As	μg L^{-1}	0.5–3.3	NM	1.14[a]	0.5[a]	3.3[a]	10
Cd	μg L^{-1}	<DL–0.1	NM	NC	<DL[a]	0.1[a]	3
Cr	μg L^{-1}	4–161.5	4–146	57.15	4	161.5	50
Cr^{6+}	μg L^{-1}	4–131.1	2–146	49.84	2	146	–
Cu	μg L^{-1}	0.2–35.5	NM	3,16[a]	0.2[a]	35.5[a]	2000
Fe	μg L^{-1}	<DL–14	NM	NC	<DL[a]	14[a]	–
Mn	μg L^{-1}	0.05–25.53	NM	2,93[a]	0.05[a]	25.53[a]	50
Ni	μg L^{-1}	0.7–21.1	NM	4,97[a]	0.7[a]	21.1[a]	70
P	μg L^{-1}	10–107	NM	26,06[a]	10[a]	107[a]	–
Pb	μg L^{-1}	<DL–2.2	NM	0,68[a]	<DL[a]	2.2[a]	10
Zn	μg L^{-1}	0.7–609.8	NM	80,99[a]	0.7[a]	609.8[a]	–

DL detection limit, *NM* not measured, *NC* not calculated

[a] Only for dataset 1

followed by Mg^{2+} ions, whereas the anionic triangle is dominated by the presence of HCO_3^{-} followed by Cl^{-} ions. The plot of geochemical data on the central diamond-shaped field, which relates cation and anion triangles, reveals that the predominant hydrochemical facies of the studied groundwater samples are Mg–Ca–HCO_3 and Mg–Ca–Cl as well as a mixed type between them. The samples were classified into two groups based on the WHO (2011) guideline value for Cr concentration for drinking water (50 μg L^{-1}). The samples having Cr ≥ 50 μg L^{-1} are marked with red circle, whereas the samples having Cr < 50 μg L^{-1} are marked with blue circles (Fig. 2).

Correlation analysis of groundwater samples

The Pearson correlation matrix of 65 groundwater samples of the Psachna basin is given in Table 3. Of statistical interest ($p < 0.01$) are the groundwater samples that presented very strong positive correlation coefficients between Cr and Cr^{6+} ($r = 0.98$), Na^{+} and Cl^{-} ($r = 0.97$), EC and TDS ($r = 0.95$), EC and Na^{+} ($r = 0.87$), EC and Cl^{-} ($r = 0.87$), and EC and Mg^{2+} ($r = 0.82$); strong positive correlation coefficients between Mg^{2+} and SO_4^{2-} ($r = 0.61$), NO_3^{-} and Cr ($r = 0.65$), and NO_3^{-} and Cr^{6+} ($r = 0.65$); and moderate positive correlation coefficients between EC and NO_3^{-} ($r = 0.47$), TDS and NO_3^{-} ($r = 0.48$), Mg^{2+} and Cr ($r = 0.53$), Mg^{2+} and Cr^{6+} ($r = 0.55$), and SO_4^{2-} and NO_3^{-} ($r = 0.51$).

Spatial distribution maps

Figure 3 presents spatial distribution maps of the concentrations of Cl^{-}, Mg^{2+}, NO_3^{-}, and Cr^{6+} for the 65 groundwater samples in the Psachna basin. The classification of different groups on the maps is symbolized by green circles,

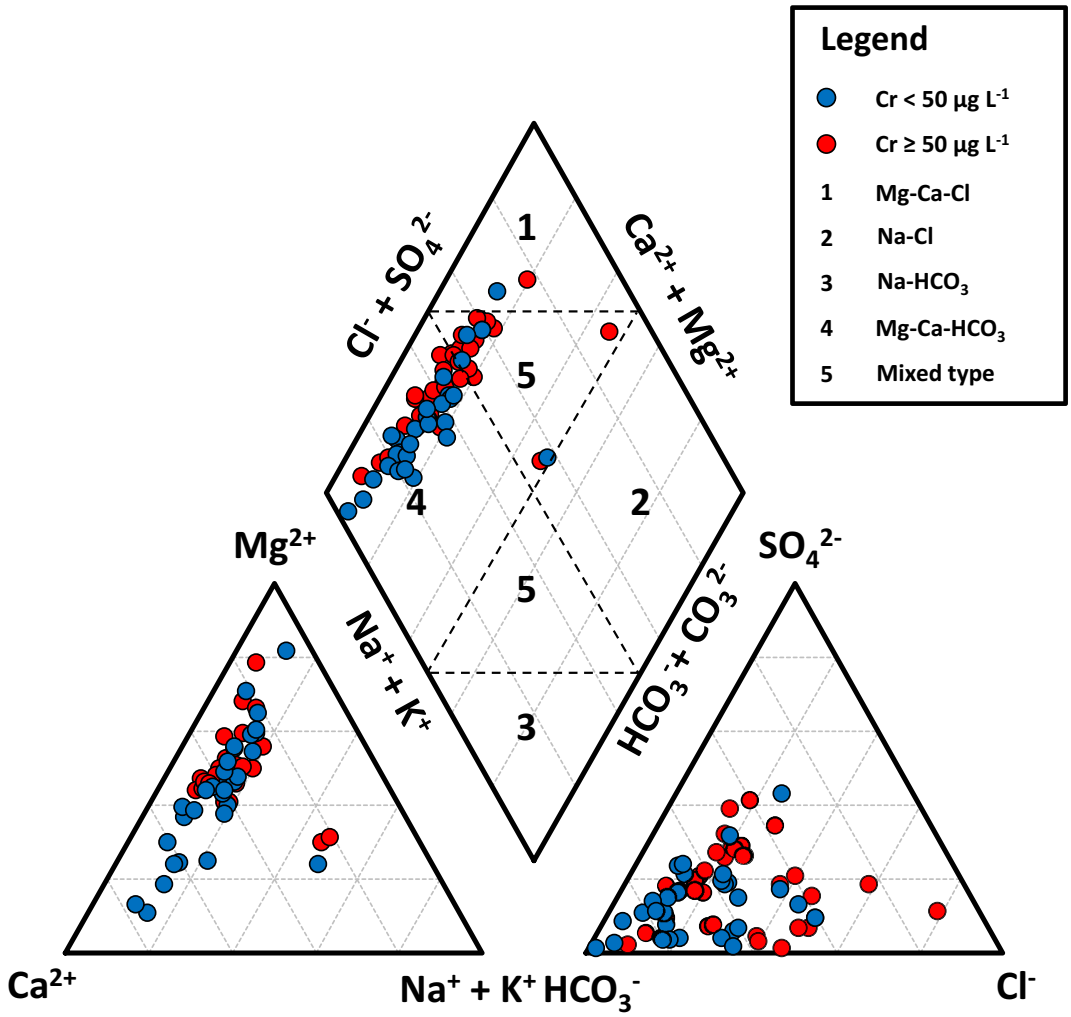

Fig. 2 Piper plot (Piper 1944) of major ion chemistry for the groundwater samples of the Psachna basin (analyzed herein)

blue squares, orange diamonds, and red triangles from lower to higher concentration. The Cl^- distribution map (Fig. 3a) shows that the highest concentrations are observed along the coastline. Concentrations of Mg^{2+} (Fig. 3b) are high in the coastal zone and exhibit an enrichment in the central part of the Psachna basin. NO_3^- (Fig. 3c) and Cr^{6+} (Fig. 3d) exhibit similar patterns with high concentrations situated in the central part of the study area and a notable enrichment in the NW.

Multivariate statistical analyses

Factor analysis

To identify the dominant factors affecting the hydrochemistry in the Psachna basin, 12 parameters, i.e., EC, pH, Ca^{2+}, Mg^{2+}, K^+, Na^+, Cl^-, SO_4^{2-}, HCO_3^-, NO_3^-, Cr, and Cr^{6+}, were analyzed to obtain the principal components for the 65 groundwater samples. As, Cd, Co, Cu, Fe, Mn, Ni, P, Pb, and Zn were excluded from processing since their concentrations were not available in the second dataset; TDS was not included either, since EC and TDS are highly dependent parameters (Obiefuna and Orazulike 2011). The Varimax orthogonal rotation with KMO normalization was used to extract the principal components. Three components having eigenvalues higher than 1 are the principal components extracted as shown in Table 4. The three factors explain 72.719% of the total variance of data. The KMO coefficient is 0.636 indicating that the results are statistically significant. Besides, the value of Bartlett's test of sphericity is < 0.05 showing that data are valid and suitable for FA.

Table 3 Pearson correlation matrix and *p* values for the groundwater analyses of the Psachna basin ($N = 65$)

Parameter	pH	EC	TDS	Ca^{2+}	Mg^{2+}	Na^{+}	K^{+}	HCO_3^{-}	SO_4^{2-}	Cl^{-}	NO_3^{-}	Cr_{tot}	Cr^{6+}
pH	1												
EC	−0.10	1											
TDS	−0.15	0.95**	1										
Ca^{2+}	−0.43**	0.73**	0.71**	1									
Mg^{2+}	−0.04	0.82**	0.78**	0.46**	1								
Na^{+}	0.05	0.87**	0.82**	0.62**	0.51**	1							
K^{+}	0.05	0.32*	0.30*	0.05	0.21	0.24	1						
HCO_3^{-}	−0.29*	0.00	0.25*	−0.02	0.03	−0.04	−0.09	1					
SO_4^{2-}	−0.06	0.67**	0.70**	0.44**	0.61**	0.46**	0.17	0.00	1				
Cl^{-}	0.09	0.87**	0.80**	0.64**	0.54**	0.97**	0.27*	−0.12	0.42**	1			
NO_3^{-}	−0.14	0.47**	0.48**	0.37**	0.66**	0.08	0.35*	−0.16	0.51**	0.11	1		
Cr_{tot}	0.14	0.39**	0.38**	0.26*	0.53**	0.16	0.29*	−0.19	0.34**	0.21	0.65**	1	
Cr^{6+}	0.14	0.42**	0.40**	0.28*	0.55**	0.20	0.25*	−0.18	0.31*	0.25*	0.65**	0.98**	1

**Correlation is significant at the 0.01 level (2-tailed)

*Correlation is significant at the 0.05 level (2-tailed)

The first factor (FA1) explains 42.626% of the total variance and includes with strong positive loadings the parameters of Na^{+} (0.966), Cl^{-} (0.966), and EC (0.896); with moderate positive loadings the parameters of Ca^{2+}

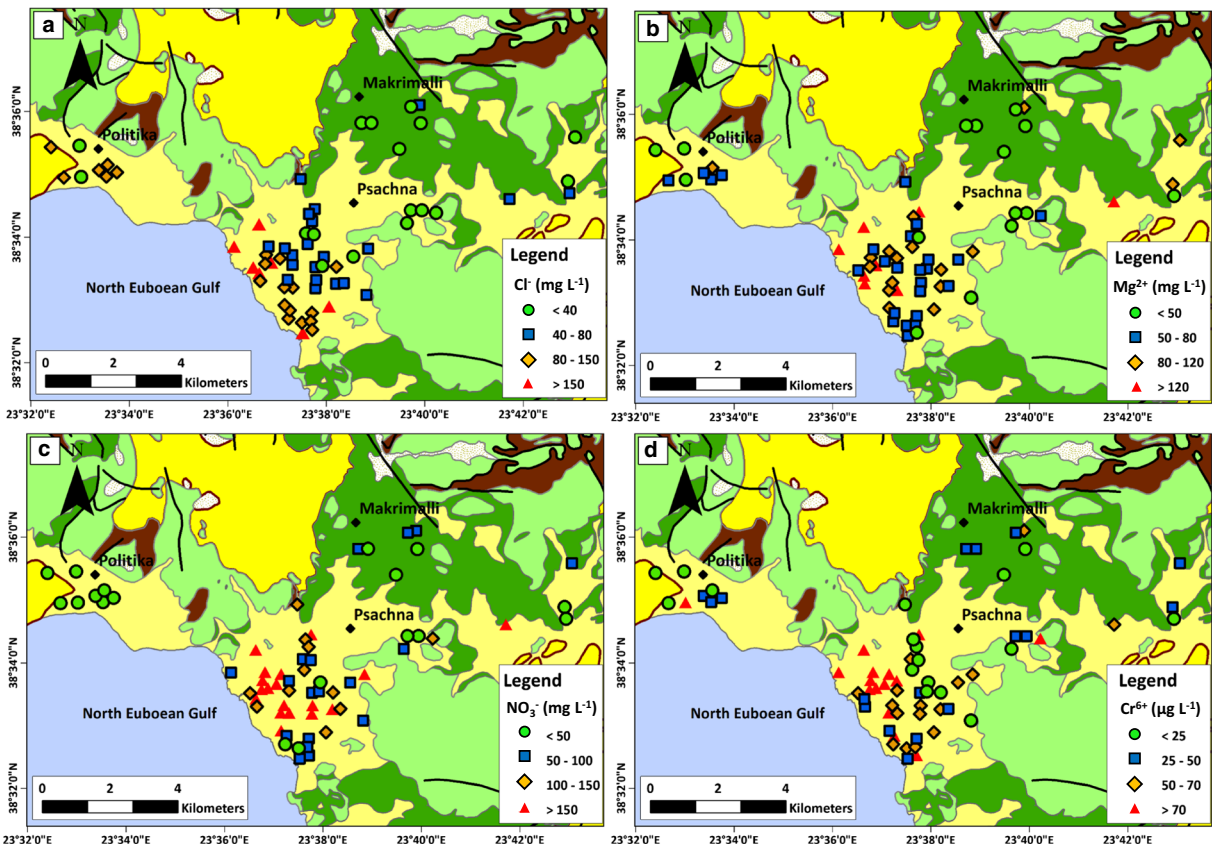

Fig. 3 Spatial distribution maps of **a** Cl^{-}, **b** Mg^{2+}, **c** NO_3^{-}, and **d** Cr^{6+} for the groundwater samples of the Psachna basin (analyzed herein)

Table 4 Varimax rotated principal components analysis for the groundwater samples in the Psachna basin

Parameter	Component		
	1	2	3
EC	0.896	0.413	− 0.047
pH	− 0.061	− 0.062	0.836
Ca^{2+}	0.722	0.272	− 0.341
Mg^{2+}	0.550	0.647	− 0.054
Na^{+}	0.966	0.038	0.111
K^{+}	0.242	0.260	0.294
HCO_3^{-}	− 0.021	− 0.095	− 0.633
SO_4^{2-}	0.329	0.622	− 0.230
Cl^{-}	0.966	0.060	0.191
NO_3^{-}	0.091	0.888	− 0.122
Cr	0.076	0.877	0.300
Cr^{6+}	0.111	0.857	0.303
Initial eigenvalues of variances in %	42.626	17.337	12.756
Cumulative % of variance	42.626	59.963	72.719

(0.722) and Mg^{2+} (0.550); and with weak positive loadings the parameter of SO_4^{2-} (0.329). The second factor (FA2) explains 17.337% of the total variance and includes with strong positive loadings the parameters of NO_3^{-} (0.888), Cr (0.877), and Cr^{6+} (0.857); with moderate positive loading the parameters of Mg^{2+} (0.647) and SO_4^{2-} (0.622); and with weak positive loading the parameter of EC (0.413). The third factor (FA3) explains 12.756% of the total variance and includes with strong positive loading the parameter of pH (0.836), with moderate negative loading the parameter of HCO_3^{-} (− 0.633), with weak positive loadings the parameters of Cr^{6+} (0.303) and Cr (0.300), and with weak negative loading the parameter of Ca^{2+} (− 0.341).

Hierarchical cluster analysis

The groundwater samples were classified into three main clusters by HCA as presented in dendrogram and spatial distribution map of Fig. 4. Samples with rescaled distance less than nine were grouped in the same cluster in order to separate sample groups with similar hydrochemical characteristics. Cluster 1 contains 20 samples, cluster 2 contains 44 samples, and cluster 3 contains only one sample. Cluster 1 includes samples characterized by higher concentrations of Ca^{2+}, Mg^{2+}, NO_3^{-}, Cl^{-}, SO_4^{2-}, Cr, and Cr^{6+} than the samples of cluster 2 (Table 5). One sample which belongs to cluster 3 exhibits very high concentrations of Cl^{-} and Na^{+}.

Soil geochemistry

In order to investigate the soil geochemistry of the Psachna basin, 16 topsoil samples (5–20 cm) were collected and analyzed (Table 6). The content of Cr ranged from 1081 to 2196.3 mg kg^{-1} (mean 1598.9 mg kg^{-1}), of Ni from 599 to 1625 mg kg^{-1} (mean 877.5 mg kg^{-1}), and of Co from 38.5 to 88.1 mg kg^{-1} (mean 53 mg kg^{-1}), indicating the weathering of ultramafic rocks. The content of P ranged from 436.4 to 2444 mg kg^{-1} (mean 1156.6 mg kg^{-1}) showing the impact of the use of P-bearing fertilizers.

Correlation analysis of soil samples

The Pearson correlation matrix of the topsoil samples of the Psachna basin is given in Table 7. Of statistical interest ($p < 0.01$) are the topsoil samples that presented very strong positive correlation coefficient of Co–Ni ($r = 0.97$) and strong positive correlation coefficients between As and Cu ($r = 0.76$), P and Zn ($r = 0.75$), Cr and Ni ($r = 0.63$), and Co and Cr ($r = 0.63$).

Discussion

Hydrochemical characteristics of groundwater

Neutral to alkaline conditions of groundwater are indicated by the measured pH values which are within the guidelines values of 6.5–8.5 for drinking water (WHO 2011). Such conditions are typical of aquifers related to ultramafic and carbonate rocks (Barnes and O'Neil 1969; Neal and Stanger 1983; Margiotta et al. 2012). EC, which is a measure of ionic strength of natural water, is below 1500 μS cm^{-1} in the majority of samples. EC exhibits statistically significant ($p < 0.01$) moderate to strong correlation coefficients with the majority of the major ions (Table 3) due to the presence of dissolved salts and the proximity of the study area to the sea. The highest concentration of Cl^{-} was observed along the coastline (Fig. 3a), indicating a seawater intrusion regime possibly due to aquifer overpumping for covering irrigational needs and the very low thickness of the UZ.

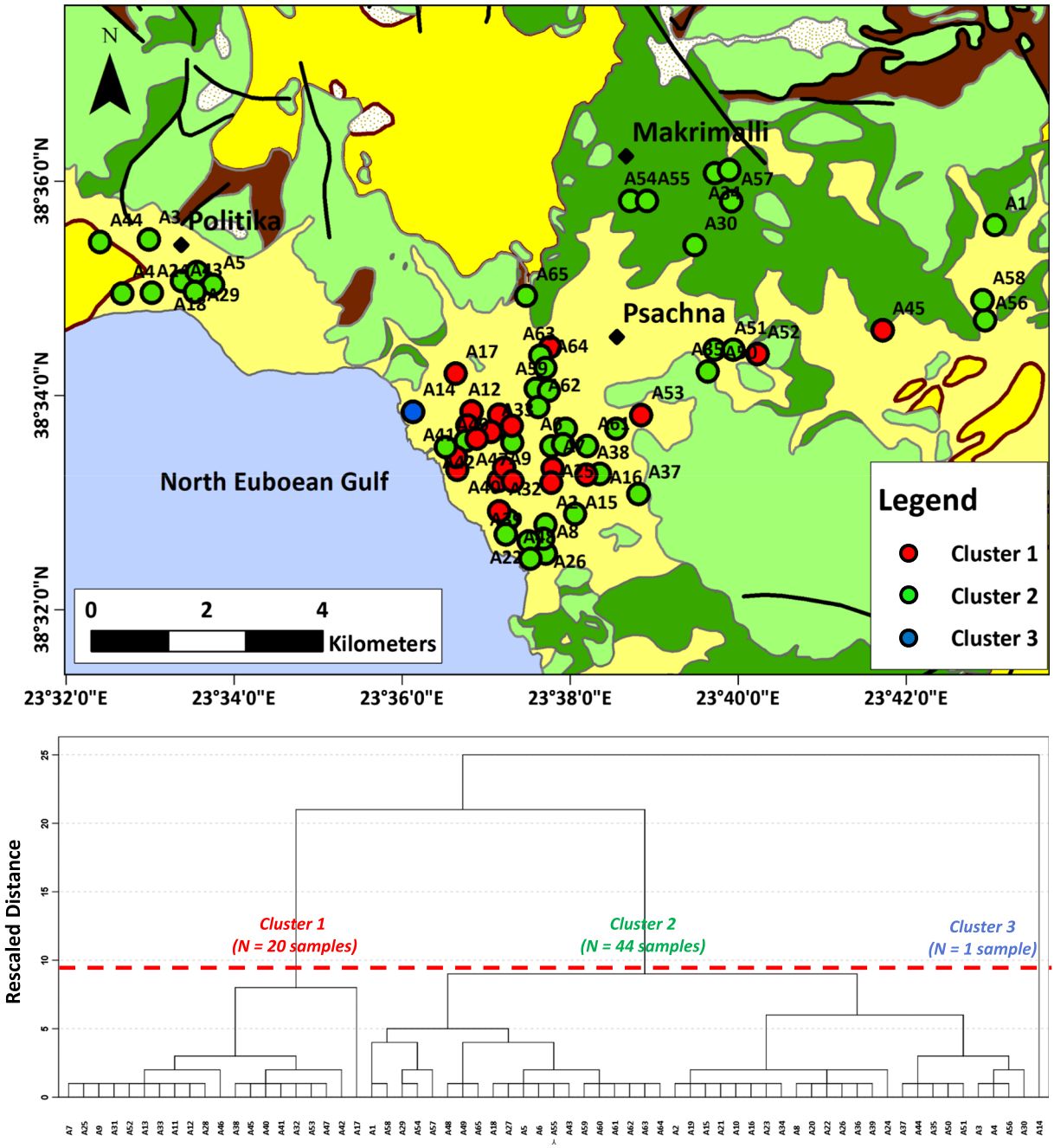

Fig. 4 Dendrogram and spatial distribution map of main clusters for the groundwater samples of the Psachna basin (analyzed herein)

The distribution patterns of major ions show compositional variation in the groundwater samples. As shown in Fig. 5a, the concentration of cations and anions, according to median value, decreases in order of abundance $Ca^{2+} > Mg^{2+} > Na^{+} > K^{+}$ and $HCO_3^{-} > NO_3^{-} > SO_4^{2-} > Cl^{-}$, respectively.

Two hydrochemical types prevail in the Psachna basin, namely the Mg–Ca–HCO_3 and the Mg–Ca–Cl, showing that groundwater quality has been affected by natural recharge and salinization, respectively.

The most remarkable characteristic in the study area is the groundwater deterioration from NO_3^{-}, Cr, and

Table 5 Descriptive statistics of the three main clusters of HCA

Parameter	Unit	Cluster 1 ($N = 20$ samples)			Cluster 2 ($N = 44$ samples)			Cluster 3 ($N = 1$ sample)		
		Mean	Min	Max	Mean	Min	Max	Mean	Min	Max
pH	–	7.41	7.15	7.61	7.54	6.8	8.27	7.71	–	–
EC	μS cm^{-1}	1554.85	1069	2481	1000.11	334	1810	5129	–	–
TDS	mg L^{-1}	1109.49	829.28	1743.7	758.22	197.62	1295.4	3237.32	–	–
Ca^{2+}	mg L^{-1}	117.33	82.5	197.58	80.88	4.48	147.38	268	–	–
Mg^{2+}	mg L^{-1}	106.21	66.8	175	58.25	7.78	116	208	–	–
Na^{+}	mg L^{-1}	48.59	24.9	99.5	38.58	9.3	186.8	604	–	–
K^{+}	mg L^{-1}	3.59	0.86	26.2	2.98	0.57	16.5	4.82	–	–
HCO_3^{-}	mg L^{-1}	334.69	246	484.34	380.01	129	976	322	–	–
SO_4^{2-}	mg L^{-1}	140.08	28.71	315	58.71	5.33	185	285	–	–
Cl^{-}	mg L^{-1}	105.1	39	369	72.89	8	294	1460	–	–
NO_3^{-}	mg L^{-1}	253.91	76	540	66.71	4.7	159	85.5	–	–
Cr	μg L^{-1}	89.54	45.2	161.5	41.83	4	89.1	83.89	–	–
Cr^{6+}	μg L^{-1}	78.15	35.05	146	36.2	2	80.65	83.89	–	–

Cr^{6+}. The concentrations of NO_3^{-} are high (mean value 124.60 mg L^{-1}), especially in the NW part of the study area (Fig. 3c), and 72.3% of collected samples exceeded the maximum permissible level for drinking water (50 mg L^{-1}, WHO 2011). NO_3^{-} are very mobile in groundwater (Hem 1985); they generally result from industrial wastewater discharges, urban domestic sewage, septic systems, human waste lagoons, animal feedlots, and animal wastes as well as the use of N-bearing fertilizers (Panno et al. 2006; Zhang et al. 2014), through complex processes such as nitrification (Weng et al. 2017), which take place in the UZ, especially in the soil, according to the following equation:

$$NH_4^{+} + 2O_2 \rightarrow NO_3^{-} + 2H^{+} + H_2O$$

The Psachna basin is characterized by intense agricultural activities accompanied by extensive use of N-bearing fertilizers that could result in the high concentrations of NO_3^{-} (up to 540 mg L^{-1}) in groundwater.

The concentrations of Cr and Cr^{6+} reach up to 161.5 and 146 μg L^{-1}, respectively. Cr^{6+}/Cr ratio is high, with values ranging between 0.5 and 1; the statistically significant ($p < 0.01$) very strong positive correlation coefficient (0.98) between these two parameters indicates that Cr^{6+} is the predominant form of Cr in groundwater (Fig. 5b), as also stated in previous studies (Megremi 2010a; Economou-Eliopoulos et al. 2014). More than half (52.3%) of the groundwater samples analyzed herein exceed the limit of 50 μg L^{-1} for Cr concentration in drinking water (WHO 2011). The origin of Cr and Cr^{6+} in groundwater is mainly geogenic attributed to the presence of ultramafic rocks and soils with Cr-bearing minerals such as chromite, serpentine, chlorite, magnetite, and Fe-hydroxides (Megremi 2010a; Voutsis et al. 2015; Economou-Eliopoulos et al. 2017). The highest concentration of Cr^{6+} was recorded in the sampling sites that the highest concentration of NO_3^{-} was recorded, too (Fig. 3c, d), indicating a possible link between these two parameters, which is discussed in detail below.

The concentrations of Cd, Co, Cu, Fe, Ni, Pb, and Zn in the groundwater samples analyzed herein are all below the guideline values of WHO (2011), due to the low solubility and mobility of these elements in geochemical conditions such as those prevailing in the study area (Hermann and Neumann-Mahlkau 1985; Smith and Huyck 1999). The concentration of Mn is up to 25.53 μg L^{-1}. The speciation of Mn in aquatic environment, controlled by the prevailing physical and chemical conditions, includes two oxidation states, the soluble Mn^{2+} and the insoluble Mn^{4+} (Homoncik et al. 2010). Given that manganese oxides were found in the form of birnessite, asbolane, and cryptomelane in the Euboea soils (Economou-Eliopoulos et al. 2014), it might be presumed that dissolved Mn^{2+} in Euboea groundwater is indicative of Cr^{3+} oxidation according to the following equation (Bartlett and James 1979; Eary and

Table 6 Sampling site coordinates and content for topsoil (5–20 cm) samples ($N = 16$) of the Psachna basin. SiO_2, Al_2O_3, Fe_2O_3, MgO, CaO, Na_2O, K_2O, TiO_2, P_2O_5, MnO, and Cr_2O_3 in weight percent; As, Cd, Co, Cu, Ni, Pb, and Zn in milligrams per kilogram. For comparison reasons, Cr and P are also given in milligrams per kilogram after conversion from Cr_2O_3 and P_2O_5% content, respectively

ID	*X*	*Y*	SiO_2 %	Al_2O_3 %	Fe_2O_3 %	MgO %	CaO %	Na_2O %	K_2O %	TiO_2 %	P_2O_5 %	MnO %	Cr_2O_3 %	As mg kg^{-1}	Cd mg kg^{-1}	Co mg kg^{-1}	Cr mg kg^{-1}	Cu mg kg^{-1}	Ni mg kg^{-1}	P mg kg^{-1}	Pb mg kg^{-1}	Zn mg kg^{-1}
E1	23° 36′ 38.325″ E	38° 33′ 26.267″ N	45.3	7.28	5.49	6.77	13.7	0.64	1.24	0.4	0.23	0.11	0.16	9.8	0.3	40.6	1081	28.6	650	1003.8	13.3	56
E2	23° 36′ 49.092″ E	38° 33′ 37.139″ N	40.11	5.89	4.95	7.34	18.54	0.5	0.95	0.32	0.22	0.09	0.17	7.8	0.3	39.6	1176.8	25.8	671	960.1	11.3	60
E3	23° 36′ 57.253″ E	38° 33′ 48.715″ N	42.49	4.96	6.83	8.33	15.94	0.43	0.79	0.27	0.16	0.11	0.31	11.1	0.2	62.3	2086.8	42.1	1120	698.3	11	45
E4	23° 37′ 23.892″ E	38° 34′ 7230″ N	46.74	7.59	6.32	8.25	11.32	0.63	1.2	0.42	0.16	0.12	0.23	9.4	0.3	52.2	1580.5	26.5	808	698.3	23.2	61
E5	23° 37′ 0.271″ E	38° 34′ 11.890″ N	35.54	2.47	5.77	16.89	15.39	0.14	0.34	0.11	0.1	0.1	0.27	2.7	0.1	66.2	1854.2	13.5	1305	436.4	6.8	39
E6	23° 36′ 10.187″ E	38° 34′ 3904″ N	35.3	5.71	7.66	7.34	17.86	0.25	0.87	0.34	0.31	0.15	0.32	8.5	0.2	76.2	2196.3	34.2	1282	1352.9	17.1	72
E7	23° 36′ 46.012″ E	38° 34′ 12.200″ N	42.88	7.15	9.16	8.58	9.92	0.34	0.95	0.44	0.29	0.16	0.26	10.8	0.3	88.1	1758.4	39.2	1625	1265.6	18.7	71
E8	23° 37′ 36.380″ E	38° 33′ 57.666″ N	44.08	7.45	5.96	6.59	14.47	0.59	1.28	0.41	0.29	0.12	0.22	10.7	0.3	44.7	1532.6	35.1	694	1265.6	17.3	78
E9	23° 37′ 15.747″ E	38° 33′ 36.415″ N	44.96	8.49	6.45	7.46	11.8	0.62	1.39	0.47	0.29	0.13	0.18	10.6	0.3	51.6	1231.6	33.9	816	1265.6	17.1	76
E10	23° 37′ 10.634″ E	38° 33′ 10.898″ N	46.12	6.3	5.58	7.57	13.75	0.54	1.06	0.35	0.24	0.1	0.24	8	0.3	45.3	1635.2	21.9	726	1047.4	12.5	64
E11	23° 37′ 51.392″ E	38° 33′ 31.143″ N	48.54	8.24	6.54	6.7	12.19	0.61	1.4	0.45	0.36	0.13	0.24	11	0.3	51.6	1648.9	30.4	782	1571.1	17.9	71
E12	23° 37′ 45.049″ E	38° 32′ 55.079″ N	45	5.9	5.31	6.5	15.72	0.54	1.03	0.33	0.37	0.11	0.24	9.8	0.3	41.2	1648.9	36.5	652	1614.8	52.7	68
E13			47.35	8.52	6.26	6.42	11.99	0.65	1.38	0.47	0.17	0.12	0.21	10.3	0.3	48.4	1464.2	26.7	729	741.9	17.2	62

Table 6 (continued)

ID	X	Y	SiO_2 %	Al_2O_3 %	Fe_2O_3 %	MgO %	CaO %	Na_2O %	K_2O %	TiO_2 %	P_2O_5 %	MnO %	Cr_2O_3 %	As mg kg^{-1}	Cd mg kg^{-1}	Co mg kg^{-1}	Cr mg kg^{-1}	Cu mg kg^{-1}	Ni mg kg^{-1}	P mg kg^{-1}	Pb mg kg^{-1}	Zn mg kg^{-1}
	23° 38′ 21.095″ E	38° 33′ 56.833″ N																				
E14	23° 37′ 8430″ E	38° 34′ 0.658″ N	41.02	5.65	5.63	8.97	16.19	0.43	0.98	0.31	0.56	0.11	0.24	6.8	0.2	49.8	1635.2	25.8	860	2444	16	77
E15	23° 38′ 52.708″ E	38° 32′ 48.993″ N	34.8	6.79	5.65	5.25	21.28	0.33	1.19	0.37	0.18	0.13	0.20	10.1	0.2	51.8	1334.2	23	721	785.6	18.9	52
E16	23° 37′ 49.689″ E	38° 33′ 8590″ N	42.25	5.08	4.88	6.09	19.02	0.5	0.84	0.29	0.31	0.09	0.25	8.2	0.4	38.5	1717.3	24.2	599	1352.9	31.4	60
Mean			42.66	6.47	6.15	7.82	149.425	0.48	1.06	0.36	0.27	0.12	0.23	9.1	0.3	53	1598.9	29.2	877.5	1156.6	18.9	63.3
Min			34.80	2.47	4.88	5.25	9.92	0.14	0.34	0.11	0.1	0.09	0.16	11.1	0.1	38.5	1081	13.5	599	436.4	6.8	39
Max			48.54	8.52	9.16	16.89	21.28	0.65	1.4	0.47	0.56	0.16	0.32	2.7	0.4	88.1	2196.3	42.1	1625	2444	31.4	78

Rai 1987; Richard and Bourg 1991; Fendorf and Zasoski 1992).

$$Cr^{3+} + 1.5\,\delta\text{–}MnO_2(s) + H_2O \rightarrow HCrO_4^- + 1.5Mn^{2+} + H^+$$

The highest concentration of P is up to 107 μg L^{-1}; P is highly immobile in soils and hardly transported into groundwater since it tends to be sorbed in minerals (Holman et al. 2008). However, statistically significant ($p < 0.01$) moderate positive correlation coefficient ($r = 0.51$) between P and Cr in groundwater of the Psachna basin was observed (Fig. 6), possibly suggesting a link between elevated concentration of Cr and agricultural activities since they result in soil enrichment in Cr (Petrotou et al. 2012; Kelepertzis 2014).

Dominant hydrochemical processes affecting groundwater quality

The hydrochemical characteristics of the groundwater of the Psachna basin show that geogenic (water–rock interaction) and anthropogenic (seawater intrusion, agriculture) influences determine the major ionic strength. Figure 7 illustrates cross plots of (a) Na^+ vs. Cl^-, (b) (Na^+/Cl^-) vs. EC, (c) ($Ca^{2+} + Mg^{2+}$) vs. Na^+, (d) chloro-alkaline indices (CAI1 and CAI2), (e) ($Ca^{2+} + Mg^{2+}$) vs. HCO_3^-, and (f) ($Ca^{2+} + Mg^{2+}$) vs. ($HCO_3^- + SO_4^{2-}$) in order to evaluate the origin of the major ions in groundwater. The linear relationship and the statistically significant ($p < 0.01$) very strong correlation coefficient ($r = 0.97$) between Na^+ and Cl^- (Fig. 7a) in the groundwater samples studied herein corroborate common origin. The majority of the groundwater samples are below the 1:1 line showing that the reverse ion exchange is the dominant geochemical process (Meybeck 1987; Zaidi et al. 2015). A limited number of samples plotted above the 1:1 line indicate that silicate dissolution has additionally affected the study area. The study area is a coastal basin and groundwater is strongly affected by seawater intrusion. The impact of seawater intrusion is further confirmed by the statistically significant ($p < 0.01$) moderate to very strong positive correlation coefficients of Cl^-–EC ($r = 0.87$), Cl^-–TDS ($r = 0.80$), Cl^-–Ca^{2+} ($r = 0.64$), Cl^-–Mg^{2+} ($r = 0.54$), and Cl^-–SO_4^{2-} ($r = 0.42$) as presented in Table 3. The physical parameters TDS and EC along with the major elements Ca^{2+}, Mg^{2+}, Na^+, Cl^-, and SO_4^{2-} tend to increase as the salinity of the groundwater increases indicating that seawater intrusion results in enrichment of these elements in groundwater. Na^+/Cl^- vs. EC cross plot is characterized by a

Table 7 Pearson correlation matrix and *p* values for the topsoil (0–20 cm) samples ($N = 16$) of the Psachna basin

Parameter	SiO_2	Al_2O_3	Fe_2O_3	MgO	CaO	Na_2O	K_2O	TiO_2	P_2O_5	MnO	Cr_2O_3	As	Cd	Co	Cu	Ni	Pb	Zn
SiO_2	1.00																	
Al_2O_3	0.65**	1.00																
Fe_2O_3	−0.02	0.22	1.00															
MgO	−0.36	−0.68**	0.08	1.00														
CaO	−0.72**	−0.52*	−0.50*	−0.13	1.00													
Na_2O	0.88**	0.75**	−0.28	−0.60*	−0.44	1.00												
K_2O	0.64**	0.96**	0.00	−0.73**	−0.38	0.81**	1.00											
TiO_2	0.62*	0.99**	0.33	−0.70**	−0.53*	0.69**	0.92**	1.00										
P_2O_5	0.14	0.13	−0.01	−0.28	0.03	0.12	0.19	0.17	1.00									
MnO	−0.06	0.45	0.87**	−0.17	−0.37	−0.18	0.30	0.54*	0.12	1.00								
Cr_2O_3	−0.30	−0.51*	0.48	0.33	0.08	−0.58*	−0.58*	−0.43	0.05	0.25	1.00							
As	0.52*	0.78**	0.35	−0.79**	−0.30	0.58*	0.75**	0.81**	0.09	0.48	−0.17	1.00						
Cd	0.67**	0.56*	−0.15	−0.67**	−0.25	0.74**	0.55*	0.59*	0.19	−0.11	−0.41	0.52*	1.00					
Co	−0.38	−0.17	0.90**	0.40	−0.26	−0.66**	−0.38	−0.07	−0.11	0.73**	0.63**	−0.04	−0.47	1.00				
Cu	0.28	0.36	0.56*	−0.43	−0.27	0.22	0.28	0.43	0.25	0.51*	0.25	0.76**	0.23	0.30	1.00			
Ni	−0.40	−0.33	0.83**	0.56*	−0.25	−0.71**	−0.53*	−0.23	−0.12	0.58*	0.64**	−0.18	−0.52*	0.97**	0.24	1.00		
Pb	0.23	0.09	−0.18	−0.39	0.08	0.24	0.14	0.13	0.36	−0.01	0.03	0.25	0.44	−0.28	0.28	−0.31	1.00	
Zn	0.36	0.58*	0.24	−0.46	−0.31	0.39	0.56*	0.63**	0.75**	0.42	−0.12	0.39	0.44	−0.03	0.42	−0.12	0.28	1.00

**Correlation is significant at the 0.01 level (2-tailed)

*Correlation is significant at the 0.05 level (2-tailed)

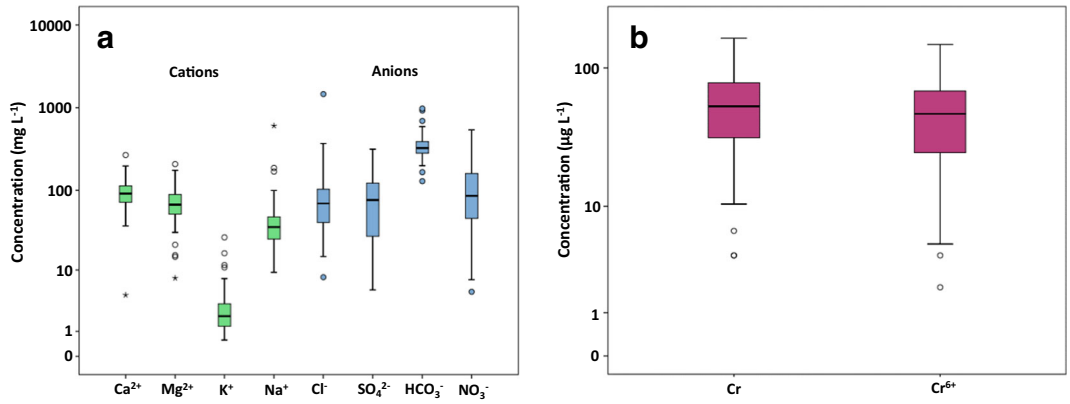

Fig. 5 **a**, **b** Boxplots showing summary data for the groundwater samples of the Psachna basin (analyzed herein)

downward inclined trend line (Fig. 7b). Besides, the (Ca^{2+} + Mg^{2+}) vs. Na^+ cross plot (Fig. 7c), in which the majority of groundwater samples are plotted above the theoretically 2:1 line, suggests the replacement of Na^+ by Ca^{2+} and/or Mg^{2+}. The decrease of Na^+/Cl^- ratio with increasing salinity (EC) combined with Na^+ removal with simultaneous increase of Ca^{2+} and/or Mg^{2+} points out that reverse ion exchange process dominates over the evaporation process in the Psachna basin. If the latter were the dominant process, a constant ratio of Na^+/Cl^- with EC increase would have been expected (Jankowski and Ian Acworth 1997; Zaidi et al. 2015). Indices of base exchange (IBE, Fig. 7d) show that 61.5% of the samples have positive values for both chloro-alkaline indices, further supporting the hypothesis that reverse ion exchange is dominant in the groundwater samples of the Psachna basin. Apart from seawater, minerals might also contribute Ca^{2+} and Mg^{2+} in the groundwater since reverse ion exchange may occur in the presence of clays with exchangeable Ca^{2+}/Mg^{2+} according to the reaction (Appelo and Postma 1996; El Yaouti et al. 2009; Fadili et al. 2015; Hounslow 2018):

$$2Na^+ + \left(Ca_{(1-y)}Mg_y\right) - X \rightarrow (1-y)Ca^{2+} + yMg^{2+} + Na_{2-X}\,(0 \le y \le 1)$$

where X indicates the exchanging solid surface.

In the plot of (Ca^{2+} + Mg^{2+}) vs. HCO_3^-, the majority of samples are above the 1:1 line (Fig. 7e), indicating

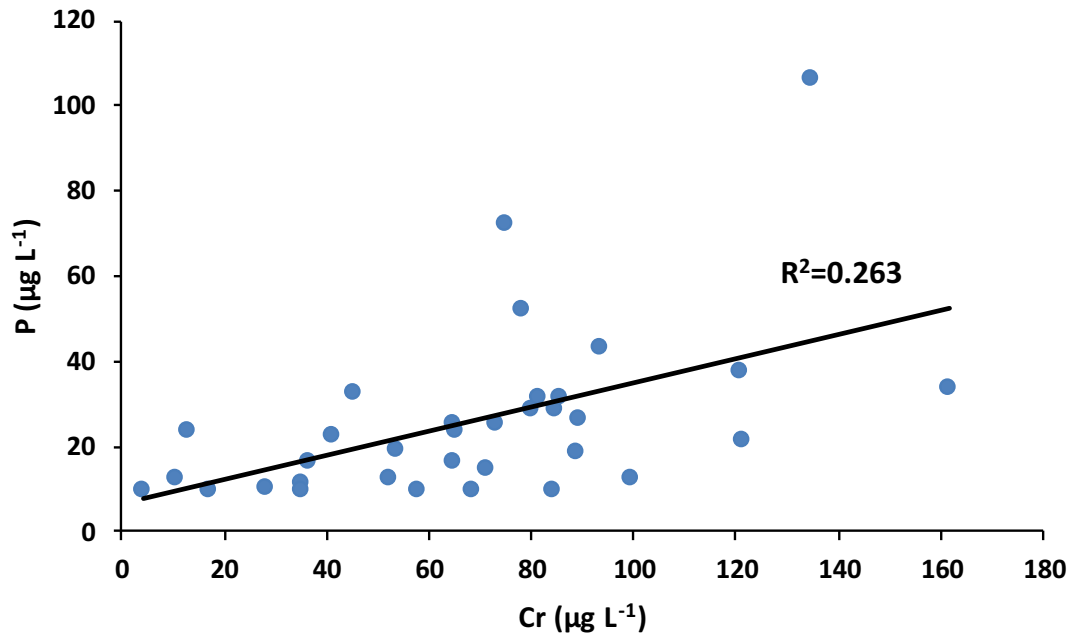

Fig. 6 Cross plot of P vs. Cr for the groundwater samples of the Psachna basin (analyzed herein)

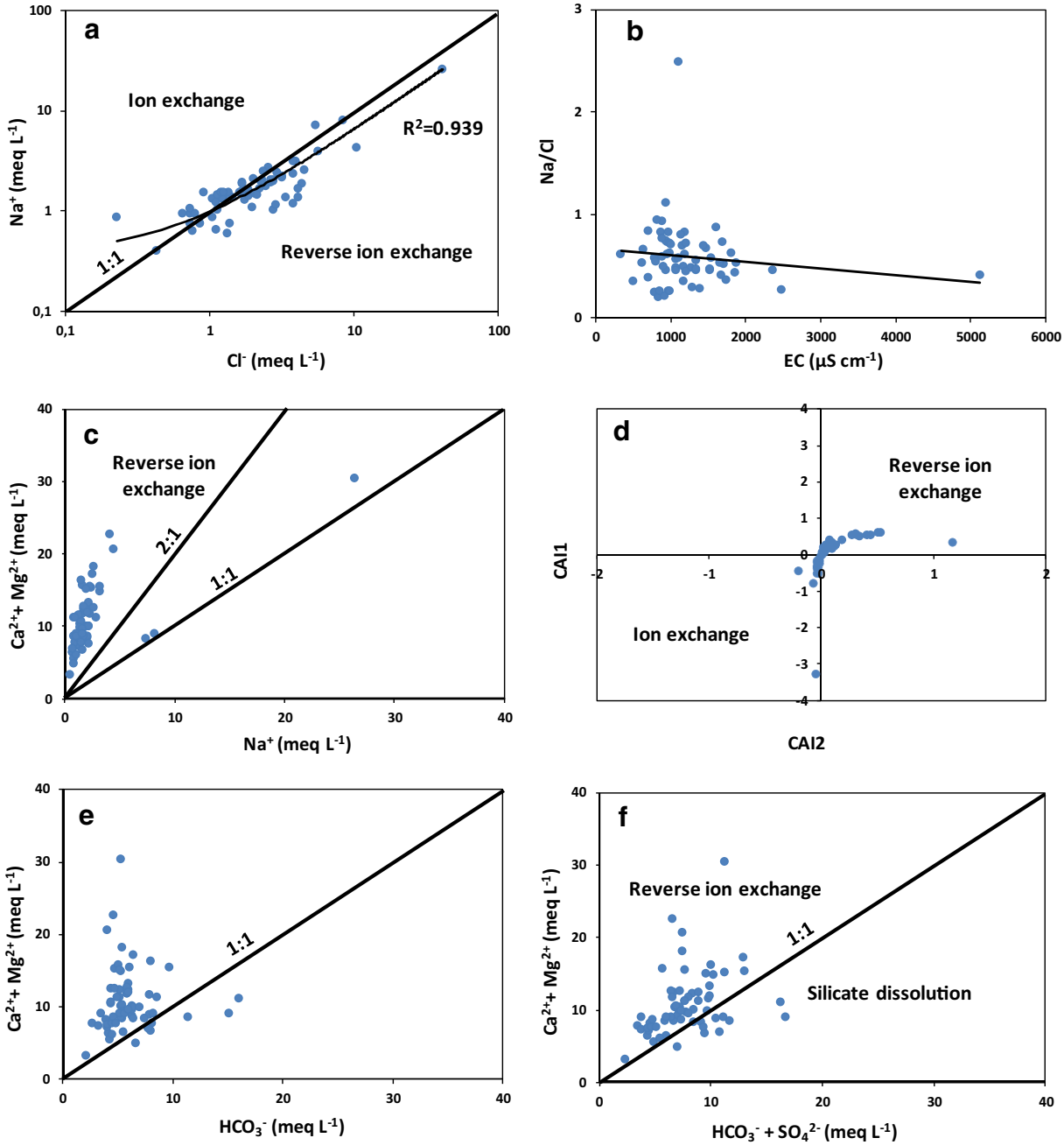

Fig. 7 Cross plots of **a** Na^+ vs. Cl^-, **b** Na^+/Cl^- vs. EC, **c** $(Ca^{2+} + Mg^{2+})$ vs. Na^+, **d** CAI1 vs. CAI2, **e** $(Ca^{2+} + Mg^{2+})$ vs. HCO_3^-, and **f** $(Ca^{2+} + Mg^{2+})$ vs. $(HCO_3^- + SO_4^{2-})$ for the groundwater samples of the Psachna basin (analyzed herein)

either the dissolution of carbonate minerals, or the reverse ion exchange process which should be balanced by SO_4^{2-} and Cl^- (Zhang et al. 1995; Singh et al. 2013). The deficiency of $(Ca^{2+} + Mg^{2+})$ relative to HCO_3^- in some samples demands that excess negative charge of bicarbonate alkalinity should be balanced by the alkalies (Na^+ or K^+) provided through water–rock interaction. Dissolution of primary silicate minerals characterized by alkaline earth metals is supported by the excess of $(HCO_3^- + SO_4^{2-})$ over $(Ca^{2+} + Mg^{2+})$ (Fig. 7f) and the simultaneous domination of HCO_3^- among the anions (Rose 2002; Rajmohan and Elango 2004; Singh et al.

2013). Carbon dioxide (CO_2) enters the water through equilibrium with the atmosphere, anoxic biodegradation of organic matter, and root respiration in the UZ (Singh et al. 2013). When dissolved in water, CO_2 (aq) readily reacts to form carbonic acid (H_2CO_3). Silicate mineral hydrolysis in the presence of H_2CO_3 occurs according to the following equation (Nesbit and Wilson 1992; Subramani et al. 2010):

$$\text{Silicate minerals} + H_2CO_3 \rightarrow \text{cations} + H_4SiO_4 + HCO_3^-$$

The very weak correlation coefficients between major ions and bicarbonates Na^+–HCO_3^- ($r = -0.04$), K^+–HCO_3^- ($r = -0.09$), Mg^{2+}–HCO_3^- ($r = 0.03$), Ca^{2+}–HCO_3^- ($r = -0.02$), and (Ca^{2+} + Mg^{2+})–HCO_3^- ($r = 0.01$) indicate that the dissolution of the carbonate minerals (magnesite, calcite and dolomite) constitutes a minor contribution to the dissolved major ions. As a result, Ca^{2+} and Mg^{2+} are mostly derived by geogenic processes such as reverse ion exchange, silicate mineral dissolution, and anthropogenic pressures mainly related to seawater intrusion. Irrigation water return flow and the use of fertilizers might additionally provide Ca^{2+} and Mg^{2+} (Menció et al. 2016).

The factors related to the origin of Cr and Cr^{6+} in groundwater of the Psachna basin were further investigated by means of multivariate statistical analyses (FA and HCA). According to FA, three factors explain the groundwater chemistry of the Psachna basin. FA1 explains 42.626% of the total variance, containing four examined parameters, i.e., EC, Na^+, Cl^-, and Ca^{2+}. FA1 is related to the increased groundwater salinization which occurs due to irrigation water return flow and seawater intrusion in the study area. The process of irrigation water return flow is common in agricultural areas such as the Psachna basin where the cumulative accumulation of corresponding ions in upper soil horizons increases salinity, especially when exploitation rate of groundwater used for irrigation is significantly higher than the recharge of aquifer systems. FA2 explains 17.337% of the total variance, containing five parameters NO_3^-, Cr, Cr^{6+}, Mg^{2+}, and SO_4^{2-}. It seems that FA2 indicates anthropogenic influences and is related to the agricultural activities due to the excessive use of N-bearing fertilizers which acts as a continuous source of N in groundwater according to previous studies (Stamatis et al. 2011; Remoundaki et al. 2016; Koilakos 2017). Figure 8 presents the spatial distribution of the scores of linear regression of FA2. The highest scores of FA2 were recorded in the sampling sites with the highest concentrations of NO_3^- and Cr^{6+} (Fig. 3c, d). The co-occurrence of NO_3^- and Cr^{6+} in the shallow aquifer (UZ ≤ 6.8 m, Gyftoulas et al. 2017) of the Psachna basin is a result of intense fertilization and irrigation water return flow (Vasileiou et al. 2014a; Manning et al. 2015; Hausladen et al. 2018).

FA3 explains 12.756% of the total variance with two parameters pH and HCO_3^- and is related with water–rock interaction reactions, thus indicating dissolution of carbonate minerals due to the hydrolysis of the HCO_3^- ion in water and/or the weathering of silicate minerals (e.g., incongruent dissolution of clays).

HCA showed that the spatial distribution of the groundwater samples of cluster 1 exhibits a similar pattern with the spatial distribution of NO_3^- and Cr^{6+} (Fig. 3c, d). Furthermore, the groundwater samples of cluster 1 have higher concentrations of Ca^{2+}, Mg^{2+}, Cl^-, SO_4^{2-}, NO_3^-, Cr, and Cr^{6+} than the groundwater samples of cluster 2, whereas the spatial distribution of cluster 1 (Fig. 4) matches with the highest regression scores of FA2 (Fig. 8) pointing the enhanced role of anthropogenic activities in groundwater quality of the study area. Cluster 3 has one sample with different hydrochemical characteristics than the rest of groundwater samples. The very high concentrations of TDS, Cl^-, and Na^+ in groundwater sample with high concentrations of Ca^{2+}, Mg^{2+}, and SO_4^{2-} indicate the direct influence of seawater intrusion.

The synergistic role of the use of fertilizers in groundwater quality in the Psachna ultramafic environment

As mentioned above, the influence of fertilization on the groundwater geochemistry of the Psachna basin is strongly recorded on the high NO_3^- concentration. Besides, the relationship between NO_3^- and other parameters, such as SO_4^{2-}, Mg^{2+}, Cr and Cr^{6+}, HCO_3^-, and TDS, further implies the role of the N-bearing fertilizers to these parameters.

More specifically:

- The statistically significant ($p < 0.01$) moderate positive correlation coefficient ($r = 0.51$) between SO_4^{2-} and NO_3^- concentrations in groundwater (Table 3, Fig. 9) indicates fertilizers as a possible source of SO_4^{2-} in groundwater in the Psachna basin.

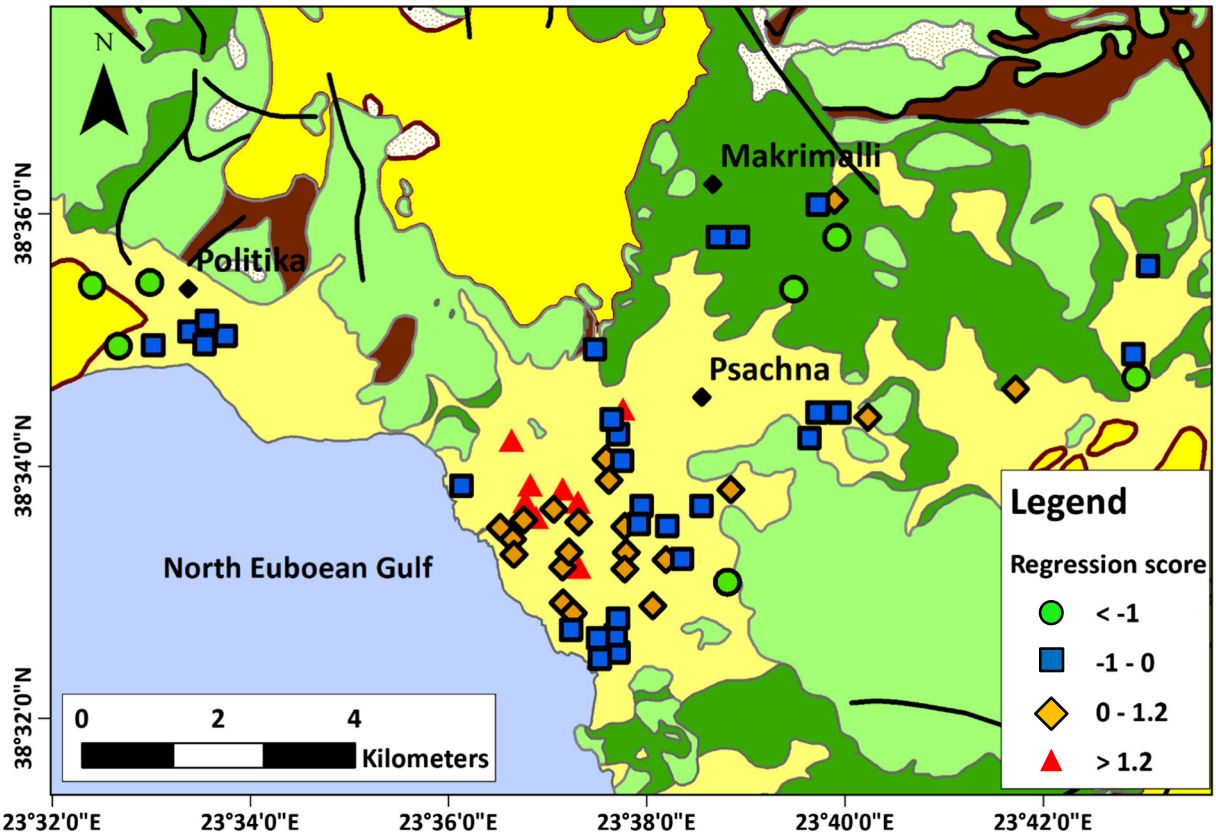

Fig. 8 Spatial distribution of individual components' contribution, according to factor 2

- The statistically significant ($p < 0.01$) strong positive correlation coefficient ($r = 0.66$) of NO_3^-–Mg^{2+} and the strong correlation coefficient ($r = 0.71$) and the linear relationship between Mg^{2+} and (Cl^- + NO_3^-) (Fig. 10) imply that the origin of Mg^{2+} in groundwater is a combined result of extensive use of agrochemical products and seawater intrusion; the domination of Mg^{2+} over (Cl^- + NO_3^-) indicates an additional minor source of Mg^{2+} in groundwater, possibly related to the interaction between Mg-rich rocks and groundwater.
- The very strong positive correlation coefficient (r = 0.81) and the linear relationship between TDS and (NO_3^- + Cl^-)/HCO_3^- (Fig. 11) reveal the influence of anthropogenic activities on water chemistry (Han and Liu 2004; Jalali 2009), especially those related with agriculture as reported in relevant studies (Barzegar et al. 2016, 2017). The persistently positive and linear relationship of TDS with the major ions (Table 3) is a further evidence of the impact of intense use of N-bearing fertilizers that results in homogenizing the contents of major dissolved ions (Menció et al. 2016) and creating a positive linear relationship between NO_3^- and major ions.
- The statistically significant ($p < 0.01$) strong positive correlation coefficients of NO_3^-–Cr ($r = 0.65$) and NO_3^-–Cr^{6+} ($r = 0.65$) (Fig. 12, Table 3) indicate the synergistic role of N-bearing fertilizers to elevated Cr^{6+} concentration in groundwater, as has been mentioned by Mills et al. (2011) and Mills and Goldhaber (2012). The proposed mechanism is that nitrification (oxidation of NH_4^+ to NO_3^-) results in the production of excess H^+ and in turn soil acidification, which favors the increased dissolution of Cr^{3+}; therefore, larger quantities of Cr^{3+} become subject to oxidation by geogenic and/or anthropogenic factors. A link between elevated Cr^{6+} concentrations and agricultural activities has been reported in previous studies in the Psachna basin (Vasileiou et al. 2014a, b; Remoundaki et al. 2016; Megremi et al. 2019) and in other similar areas as well (Stamatis et al. 2011; Papadopoulos and Lappas 2014; Dermatas et al. 2015; Koilakos 2017; Hausladen et al. 2018). NO_2^-/NO_3^- is a potential

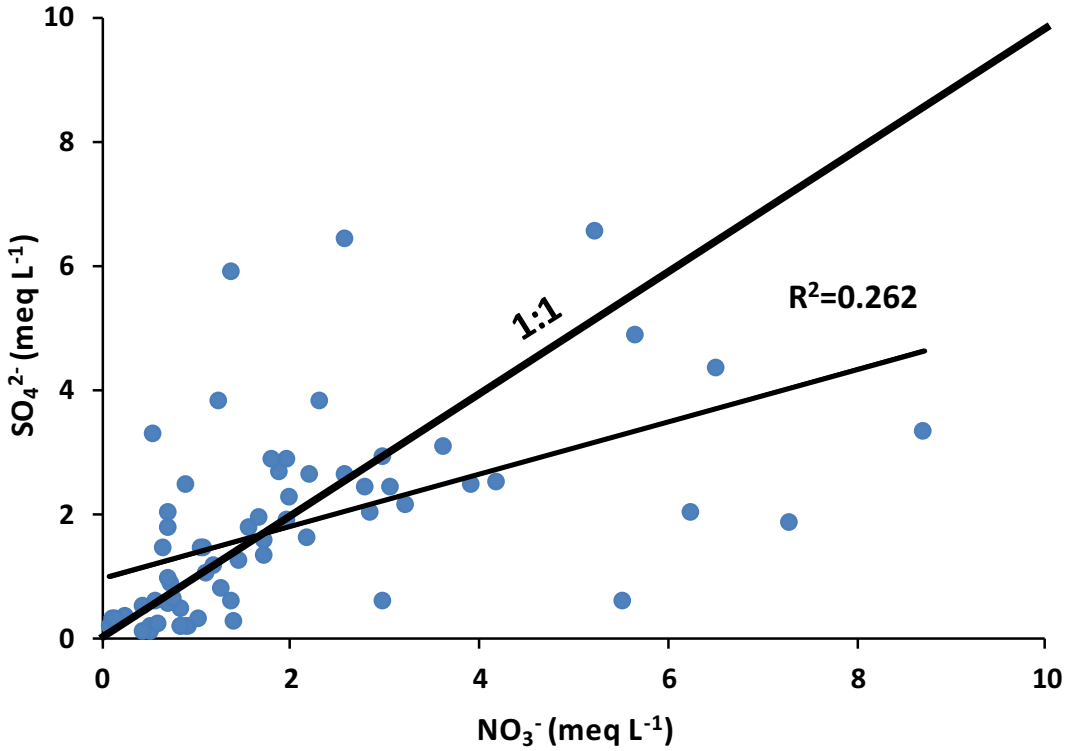

Fig. 9 Cross plot of SO_4^{2-} vs. NO_3^- for the groundwater samples of the Psachna basin (analyzed herein)

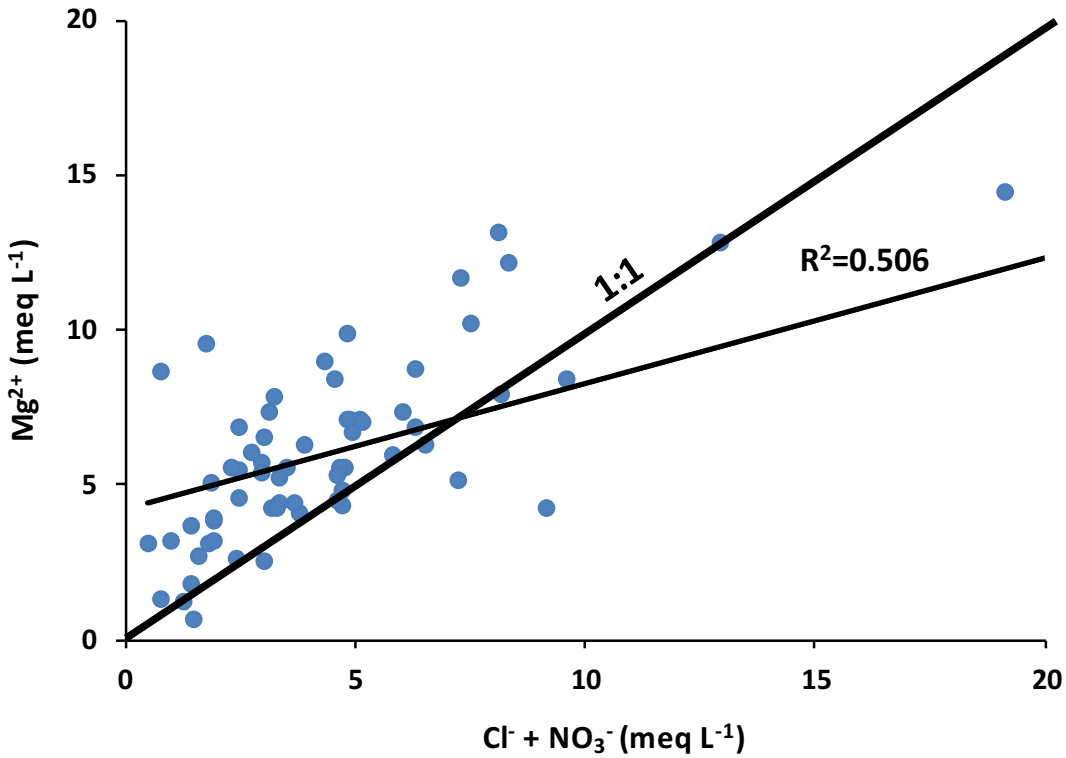

Fig. 10 Cross plot of Mg^{2+} vs. (Cl^- + NO_3^-) for the groundwater samples of the Psachna basin (analyzed herein)

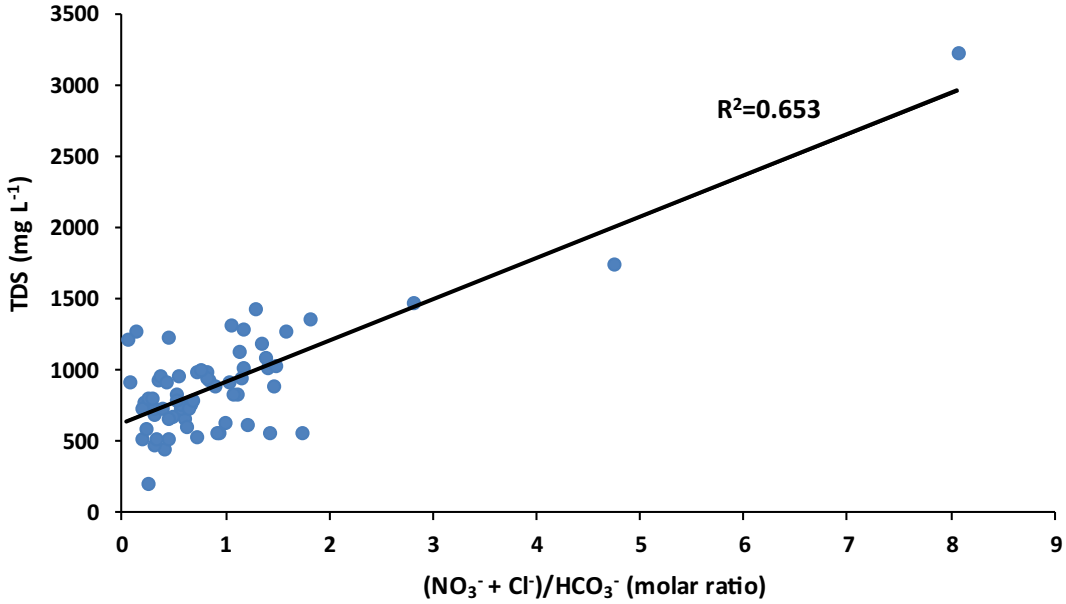

Fig. 11 Cross plot of TDS vs. $(NO_3^- + Cl^-)/HCO_3^-$ for the groundwater samples of the Psachna basin (analyzed herein)

significant redox couple which makes possible the redox transformation of Cr^{3+} into Cr^{6+} in natural aquatic environments (Richard and Bourg 1991; Stamatis et al. 2011); however, the latter has yet to explain the lower standard potential (E^0) value for NO_3^- compared to that for $Cr_2O_7^{2-}$ (Megremi et al. 2019).

In addition to N-bearing fertilizers, P-bearing fertilizers have, also, been reported to affect soil and groundwater geochemistry as they are potentially enriched in PHTE such as As, Cd, Co, Cr, Cu, Ni, Pb, and Zn (De López Camelo et al. 1997; Modaihsh et al. 2004; Chen et al. 2007; Nziguheba and Smolders 2008; Molina et al.

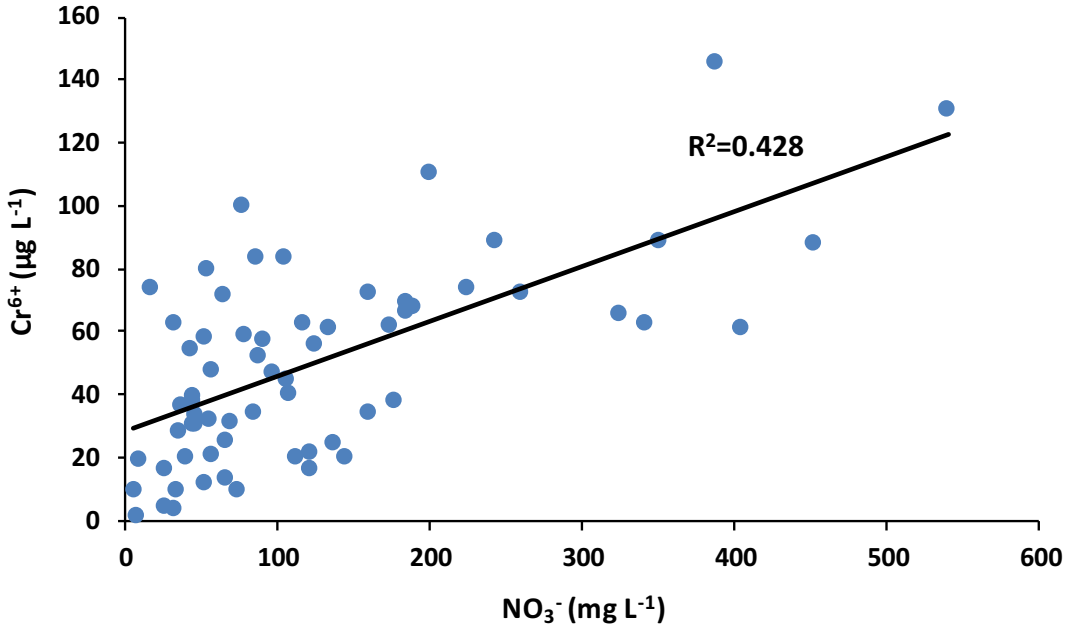

Fig. 12 Cross plot of Cr^{6+} vs. NO_3^- for the groundwater samples of the Psachna basin (analyzed herein)

2009; Cheraghi et al. 2012; Jiao et al. 2012; Nacke et al. 2013; Kelepertzis 2014; Gupta et al. 2014; Kratz et al. 2016; Krüger et al. 2017; Kourgialas et al. 2017; Da Silva et al. 2017). In Table 8, the content of selected PHTE of representative P-bearing fertilizers (P1, P2, and P3) sold and applied in a Greek market along with those fertilizers reported in previous studies worldwide is given. Besides, the mean content of PHTE in different types of P-bearing fertilizers mostly sold in Germany is presented (Table 9; Kratz et al. 2016). As can be seen, the content of each element in the fertilizers analyzed exhibits a wide range of values from nondetectable ones up to very high ones, highlighting the need of a more targeted and detailed study on the fertilizers applied in each specific area. The PHTE content of the P-bearing fertilizers varies according to the source of the phosphates even if they are of the same type (Kratz et al. 2016). The available information on the PHTE content in P-bearing fertilizers sold in Greece is very limited; a future targeted research on this direction would clarify the aforementioned issues and also contribute to the harmonization of Greek legislation with the EU directions.

The average P content in the soil samples from the Psachna basin (1156.5 mg kg^{-1}) is higher than in other areas in Greece (e.g., 554 mg kg^{-1} in Argolida, 800 mg kg^{-1} in Ptolemais-Kozani), where P in soils was attributed to the intense agricultural activities and specifically the extended use of P-bearing fertilizers (Petrotou et al. 2012; Kelepertzis 2014). Therefore, the use of P-bearing fertilizers in the Psachna basin constitutes the major source of the high content of P in soils (up to 2444 mg kg^{-1}); furthermore, it might contribute to the elevated concentrations of Cr in soils and groundwater. P-bearing fertilizers have been also considered to increase chromate desorption and, consequently, Cr^{6+} concentration in groundwater (Becquer et al. 2003).

The impact of P-bearing fertilizers in the soil geochemistry of the Psachna basin could be also documented on the elevated content of As (up to 11.1 mg kg^{-1}), Cd (up to 0.4 mg kg^{-1}), Cu (up to 42.1 mg kg^{-1}), Pb (up to 52.7 mg kg^{-1}), and Zn (up to 78 mg kg^{-1}); the aforementioned elements are in similar levels with previous reported ones in agricultural soils of Greece being related with P-bearing fertilizers (Petrotou et al. 2012; Kelepertzis 2014). The statistically significant ($p < 0.01$) strong positive correlation coefficients of P–Zn ($r = 0.75$) and As–Cu ($r = 0.76$) in soils strengthen the aforementioned hypothesis. Besides, the statistically significant ($p < 0.01$) very strong positive correlation coefficient of Co–Ni ($r = 0.97$) and the statistically significant ($p < 0.01$) strong positive correlation coefficients of Cr–

Table 8 P-bearing fertilizer content (in mg kg^{-1}) of As, Cd, Co, Cr, Cu, Ni, Pb, and Zn analyzed herein and reported in previous studies worldwide

	As	Cd	Co	Cr	Cu	Ni	Pb	Zn
P1	8.7	11.1	< 1	230	26	36	4	323
P2	20.8	< 0.1	< 0.2	< 10	0.3	0.5	< 0.1	16
P3	7.6	16.3	0.4	54.74	23.8	28.6	1.6	547
Argentina[1]	na	0–56.8	na	10.4–72.7	2.8–182.6	7–26.9	5.1–30.7	8.8–180.6
USA[2]	0–21	0–163	na	na	na	na	na	na
Brazil[3]	0.54–26.72	0.4–40.03	na	10.72–341.75	na	na	0.35–102.46	na
Saudi Arabia[4]	na	22.7–36.8	na	199.9–410	na	52.8–85.2	11.2–32.4	na
Chile[5]	8.3–19.7	2.6–57.9	1.7–3.8	66.2–924	1.5–155	1.8–17.9	3.8–22.3	28.6–883
Europe*[6]	7.6	7.4	na	89.5	na	14.8	2.9	166

na not available

*Mean values

[1] De López Camelo et al. (1997)

[2] Chen et al. (2007)

[3] Da Silva et al. (2017)

[4] Modaihsh et al. (2004)

[5] Molina et al. (2009)

[6] Nziguheba and Smolders (2008)

Table 9 Mean content of PHTE (in mg kg^{-1}) in different types of P-bearing fertilizers sold in Germany (Kratz et al. 2016)

Type of P-bearing fertilizer	As	Cd	Co	Cr	Cu	Ni	Pb	Zn
P ($n = 30$)	10.4	20.5	1.8	135	42.7	33.8	4.7	354
PK ($n = 14$)	4.2	6.7	0.83	144	16.8	20.2	4.3	173
NP ($n = 19$)	8.8	15.2	1.5	136	41.5	21.9	1.2	238
NPK ($n = 67$)	3	2.3	2.6	30.7	39	12.7	1.5	111

Ni ($r = 0.64$) and Co–Cr ($r = 0.63$) suggest the influence of the ultramafic rocks in the study area. On the other hand, the statistically insignificant ($p > 0.05$) very weak correlation coefficient of Cr–P ($r = 0.05$) implies that additional Cr from P-bearing fertilizers, although in soluble form, is very low compared to the high Cr input from ultramafic rocks and soils. However, the exact mechanism according to which P-bearing fertilizers enhance Cr mobilization has yet to be clarified. The presence of P has been linked with the desorption of the anionic Cr^{6+} sorbed on the iron oxide surfaces (Gao and Mucci 2001; Becquer et al. 2003; Zhang et al. 2004) and the subsequent release of Cr in the aquatic environment. Phosphate ions act as competitive adsorption ions with Cr^{6+} (Chowdhury and Yanful 2010). The anionic Cr^{6+} is desorbed and PO_4^{3-} are absorbed, a mechanism that explains the generally low concentrations of PO_4^{3-} in groundwaters and acts synergistically in increasing Cr mobilization in a ultramafic-dominated geological environment.

It should be mentioned here that the number of topsoil samples analyzed herein is limited and that the soil geochemistry in the present context is used in order to additionally evaluate groundwater geochemistry. Besides, for reasons of comparison with existing literature data, only topsoils were studied. A future research might focus on the detailed study of both topsoils and subsoils and the geochemical processes that take place in different soil depths with emphasis on the mobilization of PHTE of fertilizers.

Conclusions

Co-evaluating geological, geochemical, hydrogeological, and hydrochemical data for the Psachna basin, central Euboea, Greece, by means of (a) hydrochemical cross plots of major ions; (b) spatial distribution maps of Cl^-, Mg^{2+}, NO_3^-, and Cr^{6+}; and (c) multivariate statistical analyses such as factor analysis and hierarchical cluster analysis of groundwater geochemistry showed that groundwater quality is strongly affected by the ultramafic geological environment with anthropogenic activities and mainly the agricultural ones acting synergistically.

The main characteristics of the Psachna groundwaters are the alkaline pH; the two dominant hydrochemical water types, namely the Mg–Ca–HCO_3 and the Mg–Ca–Cl; and the deterioration by elevated concentrations of NO_3^-, Cr, and Cr^{6+} which in many cases exceed the maximum permitted level of 50 mg L^{-1} for drinking water (WHO 2011). The concentration of cations and anions decreases in order of abundance $Ca^{2+} > Mg^{2+} > Na^+ > K^+$ and $HCO_3^- > NO_3^- > SO_4^{2-} > Cl^-$, respectively.

The major factors that control the hydrochemistry of the study area are reverse ion exchange, dissolution of silicate minerals, and intense agricultural activities (fertilization and irrigation water return flow). According to FA, three factors explain 73.2% of the total variance of data. FA1 (salinity factor) contained high loadings of Na^+, Cl^-, EC, Ca^{2+}, SO_4^{2-}, and Mg^{2+}; FA2 (fertilization factor) contained high loadings of NO_3^-, Cr, Cr^{6+}, Mg^{2+}, SO_4^{2-}, and EC; and FA3 (water–rock interaction factor) has high loadings of pH, HCO_3^-, Ca^{2+}, Cr, and Cr^{6+}. HCA classified the groundwater samples of the study area into three main clusters separating an area in which the impact of anthropogenic activities is more intense, and the concentrations of Cr, Cr^{6+}, and NO_3^- in groundwater exhibit similar spatial distribution patterns. Strong correlation of NO_3^-–Cr and NO_3^-–Cr^{6+} in groundwater further points to the synergistic role of N-bearing fertilizers in groundwater quality and specifically the elevated concentration of Cr and Cr^{6+}. Besides, the strong positive correlation between NO_3^- and other parameters such as SO_4^{2-} and Mg^{2+} in groundwater samples and the very high content of P, up to 2444 mg kg^{-1}, in soil samples of the Psachna basin, implies the synergistic, although commonly neglected, role of the use of fertilizers in groundwater quality.

Considering all the above, the use of fertilizers seems to have a complex role in groundwater quality, the main aspects of which are as follows:

(a) The increased dissolution of geogenic Cr^{3+} due to nitrification and soil acidification caused by N-bearing fertilizers (anthropogenic factor contributing to the oxidation of geogenic Cr), a mechanism proposed by Mills et al. (2011)
(b) The increased chromate desorption caused by P-bearing fertilizers, a mechanism proposed by Becquer et al. (2003), enhancing Cr mobilization from soils to groundwater and subsequent Cr oxidation to C^{6+}
(c) The additional anthropogenic source of Cr and other PHTE from P-bearing fertilizers, although of minor contribution compared to the geogenic Cr input

The above-described impact of the use of fertilizers in groundwater geochemistry would omit its synergistic role in an environment poor in geogenic Cr; it is exactly the presence of ultramafic rocks and soils that favor the elevated concentration of Cr which is further intensified by the agricultural activities.

Future studies that focus on the exact type and quantities of the fertilizers applied to the Psachna soils, on the chemical composition of the P-bearing fertilizers with emphasis placed on PHTE as well as on the mechanism which results in elevated Cr^{6+} concentration in groundwater need to be carried out in order to elucidate their role and, subsequently, to constitute a base for applying the best practices for land use management with respect to the local agriculture-based economy.

Acknowledgments Constructive comments and suggestions by two anonymous reviewers are greatly appreciated. We thank Dr. F. Kutz for careful editorial handling. This work is part of the research project NTUA 623147.

References

Aghazadeh, N., & Mogaddam, A. A. (2011). Investigation of hydrochemical characteristics of groundwater in the Harzandat aquifer, northwest of Iran. *Environmental Monitoring and Assessment., 176*, 183–195. https://doi.org/10.1007/s10661-010-1575-4.

Appelo, C. A. J., & Postma, D. (1996). *Geochemistry, groundwater and pollution*. Rotterdam: A.A. Balkema.

Ball, J. W., & McCleskey, R. B. (2003). A new cation-exchange method for accurate field speciation of hexavalent chromium. *Talanta., 61*, 305–313. https://doi.org/10.1016/S0039-9140(03)00282-0.

Barnes, I., & O'Neil, J. R. (1969). The relationship between fluids in some fresh alpine-type ultramafics and possible modern serpentinization, western United States. *Bulletin of the Geological Society of America., 80*, 1947. https://doi.org/10.1130/0016-7606(1969)80[1947:TRBFIS]2.0.CO;2.

Bartlett, R., & James, B. (1979). Behavior of chromium in soils: III. Oxidation 1. *Journal of Environment Quality, 8*. https://doi.org/10.2134/jeq1979.00472425000800010008x.

Barzegar, R., Asghari Moghaddam, A., & Tziritis, E. (2016). Assessing the hydrogeochemistry and water quality of the Aji-Chay River, northwest of Iran. *Environmental Earth Sciences., 75*. https://doi.org/10.1007/s12665-016-6302-1.

Barzegar, R., Moghaddam, A. A., Tziritis, E., Fakhri, M. S., & Soltani, S. (2017). Identification of hydrogeochemical processes and pollution sources of groundwater resources in the Marand plain, northwest of Iran. *Environmental Earth Sciences., 76*. https://doi.org/10.1007/s12665-017-6612-y.

Becquer, T., Quantin, C., Sicot, M., & Boudot, J. P. (2003). Chromium availability in ultramafic soils from New Caledonia. *Science of the Total Environment., 301*, 251–261. https://doi.org/10.1016/S0048-9697(02)00298-X.

Bertolo, R., Bourotte, C., Hirata, R., Marcolan, L., & Sracek, O. (2011). Geochemistry of natural chromium occurrence in a sandstone aquifer in Bauru Basin, São Paulo State, Brazil. *Applied Geochemistry., 26*, 1353–1363. https://doi.org/10.1016/j.apgeochem.2011.05.009.

Bourotte, C., Bertolo, R., Almodovar, M., & Hirata, R. (2009). Natural occurrence of hexavalent chromium in a sedimentary aquifer in Uraina, state of Sao Paulo, Brazil. *Anais da Academia Brasileira de Ciencias., 81*, 227–242. https://doi.org/10.1590/S0001-37652009000200009.

Cattell, R. B. (1966). The scree test for the number of factors. *Multivariate Behavioral Research, 1*, 245–276. https://doi.org/10.1207/s15327906mbr0102_10.

Chen, W., Chang, A. C., & Wu, L. (2007). Assessing long-term environmental risks of trace elements in phosphate fertilizers. *Ecotoxicology and Environmental Safety., 67*, 48–58. https://doi.org/10.1016/j.ecoenv.2006.12.013.

Cheraghi, M., Lorestani, B., & Merrikhpour, H. (2012). Investigation of the effects of phosphate fertilizer application on the heavy metal content in agricultural soils with different cultivation patterns. *Biological Trace Element Research., 145*, 87–92. https://doi.org/10.1007/s12011-011-9161-3.

Chowdhury, S. R., & Yanful, E. K. (2010). Arsenic and chromium removal by mixed magnetite-maghemite nanoparticles and the effect of phosphate on removal. *Journal of Environmental Management., 91*, 2238–2247. https://doi.org/10.1016/j.jenvman.2010.06.003.

Cooper, G. R. C. (2002). Oxidation and toxicity of chromium in ultramafic soils in Zimbabwe. *Applied Geochemistry, 17*, 981–986. https://doi.org/10.1016/S0883-2927(02)00014-8.

da Silva, F. B. V., Williams Araújo do Nascimento, C., & Renata Muniz Araújo, P. (2017). Environmental risk of trace elements in P-containing fertilizers marketed in Brazil. *Journal of Soil Science and Plant Nutrition, 17*.

Dandolos, H., & Zorapas, B. (2010). *Recording and assessment of the underground aquifer systems of Boeotian Kifissos and the sub-elected prefecture of Viotia - Evia*. Athens: Institute of Geological and Mining Exploration (in Greek).

De López Camelo, L. G., De Miguez, S. R., & Marbán, L. (1997). Heavy metals input with phosphate fertilizers used in

Argentina. *Science of the Total Environment., 204*, 245–250. https://doi.org/10.1016/S0048-9697(97)00187-3.

Dermatas, D., Mpouras, T., Chrysochoou, M., Panagiotakis, I., Vatseris, C., Linardos, N., Theologou, E., Boboti, N., Xenidis, A., Papassiopi, N., & Sakellariou, L. (2015). Origin and concentration profile of chromium in a Greek aquifer. *Journal of Hazardous Materials., 281*, 35–46. https://doi.org/10.1016/j.jhazmat.2014.09.050.

Eary, L. E., & Rai, D. (1987). Kinetics of chromium(III) oxidation to chromium(VI) by reaction with manganese dioxide. *Environmental Science and Technology., 21*, 1187–1193. https://doi.org/10.1021/es00165a005.

Economou-Eliopoulos, M., Megremi, I., & Vasilatos, C. (2011). Factors controlling the heterogeneous distribution of Cr(VI) in soil, plants and groundwater: evidence from the Assopos basin, Greece. *Chemie der Erde., 71*, 39–52. https://doi.org/10.1016/j.chemer.2011.01.001.

Economou-Eliopoulos, M., Antivachi, D., Vasilatos, C., & Megremi, I. (2012). Evaluation of the Cr(VI) and other toxic element contamination and their potential sources: the case of the Thiva basin (Greece). *Geoscience Frontiers., 3*, 523–539. https://doi.org/10.1016/j.gsf.2011.11.010.

Economou-Eliopoulos, M., Megremi, I., Atsarou, C., Theodoratou, C., & Vasilatos, C. (2013). Spatial evolution of the chromium contamination in soils from the Assopos to Thiva Basin and C. Evia (Greece) and potential source(s): anthropogenic versus natural processes. *Geosciences.* https://doi.org/10.3390/geosciences3020140.

Economou-Eliopoulos, M., Frei, R., & Atsarou, C. (2014). Application of chromium stable isotopes to the evaluation of Cr(VI) contamination in groundwater and rock leachates from central Euboea and the Assopos basin (Greece). *Catena., 122*, 216–228. https://doi.org/10.1016/j.catena.2014.06.013.

Economou-Eliopoulos, M., Megremi, I., Vasilatos, C., Frei, R., & Mpourodimos, I. (2017). Geochemical constraints on the sources of Cr(VI) contamination in waters of Messapia (central Evia) basin. *Applied Geochemistry, 84*, 13–25. https://doi.org/10.1016/j.apgeochem.2017.05.015.

El Yaouti, F., El Mandour, A., Khattach, D., Benavente, J., & Kaufmann, O. (2009). Salinization processes in the unconfined aquifer of Bou-Areg (NE Morocco): a geostatistical, geochemical, and tomographic study. *Applied Geochemistry.* https://doi.org/10.1016/j.apgeochem.2008.10.005.

Council Directive 98/83/EC of 3 November 1998 on the quality of water intended for human consumption, L330/32.

Evans, J. D. (1996). *Straightforward statistics for the behavioral sciences*. Belmont: Thomson Brooks/Cole Publishing Co.

Fadili, A., Mehdi, K., Riss, J., Najib, S., Makan, A., & Boutayab, K. (2015). Evaluation of groundwater mineralization processes and seawater intrusion extension in the coastal aquifer of Oualidia, Morocco: hydrochemical and geophysical approach. *Arabian Journal of Geosciences., 8*, 8567–8582. https://doi.org/10.1007/s12517-015-1808-5.

Fandeur, D., Juillot, F., Morin, G., Livi, L., Cognigni, A., Webb, S. M., Ambrosi, J.-P., Fritsch, E., Guyot, F., & Brown, G. (2009). XANES evidence for oxidation of Cr(III) to Cr(VI) by Mn-oxides in a lateritic regolith developed on serpentinized ultramafic rocks of New Caledonia. *Environmental Science and Technology., 43*, 7384–7390. https://doi.org/10.1021/es900498r.

Fantoni, D., Brozzo, G., Canepa, M., Cipolli, F., Marini, L., Ottonello, G., & Vetuschi Zuccolini, M. (2002). Natural hexavalent chromium in groundwaters interacting with ophiolitic rocks. *Environmental Geology, 42*, 871–882. https://doi.org/10.1007/s00254-002-0605-0.

Faridullah, F., Umar, M., Alam, A., Sabir, M. A., & Khan, D. (2017). Assessment of heavy metals concentration in phosphate rock deposits, Hazara basin, Lesser Himalaya Pakistan. *Geosciences Journal., 21*, 743–752. https://doi.org/10.1007/s12303-017-0013-9.

Fendorf, S. E., & Zasoski, R. J. (1992). Chromium(III) oxidation by δ-manganese oxide (MnO2). 1. Characterization. *Environmental Science and Technology*. https://doi.org/10.1021/es00025a006.

Fendorf, S. E., Fendorf, M., Sparks, D. L., & Gronsky, R. (1992). Inhibitory mechanisms of Cr(III) oxidation by δ-MnO2. *Journal of Colloid and Interface Science., 153*, 37–54. https://doi.org/10.1016/0021-9797(92)90296-X.

Feng, X. H., Zhai, L. M., Tan, W. F., Liu, F., & He, J. Z. (2007). Adsorption and redox reactions of heavy metals on synthesized Mn oxide minerals. *Environmental Pollution., 147*, 366–373. https://doi.org/10.1016/j.envpol.2006.05.028.

Gao, Y., & Mucci, A. (2001). Acid base reaction, phosphate and arsenate complexation, and thier competitive adsorption at the surface of geothite in 0.7 M NaCl solution. *Geochimica et Cosmochimica Acta.* https://doi.org/10.1016/S0016-7037(01)00589-0.

Gonzalez, A. R., Ndung'u, K., & Flegal, A. R. (2005). Natural occurrence of hexavalent chromium in the Aromas Red Sands aquifer, California. *Environmental Science and Technology., 39*, 5505–5511. https://doi.org/10.1021/es048835n.

Gupta, D. K., Chatterjee, S., Datta, S., Veer, V., & Walther, C. (2014). Role of phosphate fertilizers in heavy metal uptake and detoxification of toxic metals. *Chemosphere., 108*, 134–144. https://doi.org/10.1016/j.chemosphere.2014.01.030.

Gyftoulas, A., Melas, E., Stamatis, G., & Tsiros, I. (2017). Hydrogeological and hydrochemical investigation of the aquifer system in Psachna valley (W. Evia). 11th international hydrogeological congress of Greece, 4-7 October, Athens, English volume, pp. 243–252.

Han, G., & Liu, C. Q. (2004). Water geochemistry controlled by carbonate dissolution: a study of the river waters draining karst-dominated terrain, Guizhou Province, China. *Chemical Geology., 204*, 1–21. https://doi.org/10.1016/j.chemgeo.2003.09.009.

Hausladen, D. M., Alexander-Ozinskas, A., McClain, C., & Fendorf, S. (2018). Hexavalent chromium sources and distribution in California groundwater. *Environmental Science and Technology., 52*, 8242–8251. https://doi.org/10.1021/acs.est.7b06627.

Hem, D. (1985). Study and interpretation the chemical of natural of characteristics water. USGS Science for a changing world, U.S Geological Survey Water-Supply Paper-2254. https://doi.org/10.1118/1.596347

Hermann, R., & Neumann-Mahlkau, P. (1985). The mobility of zinc, cadmium, copper, lead, iron and arsenic in ground water as a function of redox potential and pH. *The Science of the Total Environment, 43*, 1–12. https://doi.org/10.1016/0048-9697(85)90027-0.

Holman, I. P., Whelan, M. J., Howden, N. J. K., Bellamy, P. H., Willby, N. J., Rivas-Casado, M., & McConvey, P. (2008). Phosphorus in groundwater—an overlooked contributor to eutrophication? *Hydrological Processes, 22*, 5121–5127. https://doi.org/10.1002/hyp.7198.

Homoncik, S. C., Macdonald, A. M., Heal, K. V. Ó., Dochartaigh, B. É., & Ngwenya, B. T. (2010). Manganese concentrations in Scottish groundwater. *Science of the Total Environment., 408*, 2467–2473. https://doi.org/10.1016/j.scitotenv.2010.02.017.

Hounslow, A. W. (2018). Water quality data: analysis and interpretation. https://doi.org/10.1201/9780203734117.

Izbicki, J. A., Ball, J. W., Bullen, T. D., & Sutley, S. J. (2008). Chromium, chromium isotopes and selected trace elements, western Mojave Desert, USA. *Applied Geochemistry., 23*, 1325–1352. https://doi.org/10.1016/j.apgeochem.2007.11.015.

Jacobs, J., & Testa, S. M. (2004). Overview of chromium(VI) in the environment: background and history. In *Chromium Handbook* (pp. 1–21). Boca Raton: CRC Press.

Jalali, M. (2009). Geochemistry characterization of groundwater in an agricultural area of Razan, Hamadan, Iran. *Environmental Geology., 56*, 1479–1488. https://doi.org/10.1007/s00254-008-1245-9.

Jankowski, J., & Ian Acworth, R. (1997). Impact of debris-flow deposits on hydrogeochemical processes and the development of dryland salinity in the Yass River Catchment, New South Wales, Australia. *Hydrogeology Journal., 5*, 71–88. https://doi.org/10.1007/s100400050119.

Jiao, W., Chen, W., Chang, A. C., & Page, A. L. (2012). Environmental risks of trace elements associated with long-term phosphate fertilizers applications: a review. *Environmental Pollution., 168*, 44–53. https://doi.org/10.1016/j.envpol.2012.03.052.

Kaiser, H. F. (1958). The varimax criterion for analytic rotation in factor analysis. *Psychometrika., 23*, 187–200. https://doi.org/10.1007/BF02289233.

Kaitantzian, A., Kelepertzis, E., & Kelepertzis, A. (2013). Evaluation of the sources of contamination in the suburban area of Koropi-Markopoulo, Athens, Greece. *Bulletin of Environmental Contamination and Toxicology., 91*, 23–28. https://doi.org/10.1007/s00128-013-1023-6.

Kaprara, E., Kazakis, N., Simeonidis, K., Coles, S., Zouboulis, A. I., Samaras, P., & Mitrakas, M. (2015). Occurrence of Cr(VI) in drinking water of Greece and relation to the geological background. *Journal of Hazardous Materials., 281*, 2–11. https://doi.org/10.1016/j.jhazmat.2014.06.084.

Katsikatsos, G., Fytrolakis, N., & Perdikatsis, V. (1980). Contribution to the genesis of lateritic deposits of the upper Cretaceous transgression in Attica and complexes. The eastern Mediterranean–western Asia area and its comparison with similar metallogenic environments in the world. Proceedings of international symposium in metallogeny of mafic and ultramafic.

Katsikatsos, G., Koukis, G., Fytikas, M., Anastopoulos, J., & Kanaris, J. (1981). *Geological map of Greece, scale 1: 50.000, Psachna-Pilion sheet*. Rethymno: Greek Institute of Geology and Mineral Exploration.

Kazakis, N., Kantiranis, N., Voudouris, K. S., Mitrakas, M., Kaprara, E., & Pavlou, A. (2015). Geogenic Cr oxidation on the surface of mafic minerals and the hydrogeological conditions influencing hexavalent chromium concentrations in groundwater. *Science of the Total Environment., 514*, 224–238. https://doi.org/10.1016/j.scitotenv.2015.01.080.

Kelepertzis, E. (2014). Accumulation of heavy metals in agricultural soils of Mediterranean: insights from Argolida basin, Peloponnese, Greece. *Geoderma*. https://doi.org/10.1016/j.geoderma.2014.01.007.

Kelepertzis, E., Galanos, E., & Mitsis, I. (2013). Origin, mineral speciation and geochemical baseline mapping of Ni and Cr in agricultural topsoils of Thiva Valley (central Greece). *Journal of Geochemical Exploration., 125*, 56–68. https://doi.org/10.1016/j.gexplo.2012.11.007.

Koilakos, D. I. (2017). Aspects of hexavalent chromium pollution of Thebes plain aquifer, Boeotia, Greece. *Water (Switzerland)., 9*. https://doi.org/10.3390/w9080611.

Kotaś, J., & Stasicka, Z. (2000). Chromium occurrence in the environment and methods of its speciation. *Environmental Pollution., 107*, 263–283. https://doi.org/10.1016/S0269-7491(99)00168-2.

Kourgialas, N. N., Karatzas, G. P., & Koubouris, G. C. (2017). A GIS policy approach for assessing the effect of fertilizers on the quality of drinking and irrigation water and wellhead protection zones (Crete, Greece). *Journal of Environmental Management., 189*, 150–159. https://doi.org/10.1016/j.jenvman.2016.12.038.

Kožuh, N., Štupar, J., & Gorenc, B. (2000). Reduction and oxidation processes of chromium in soils. *Environmental Science and Technology., 34*, 112–119. https://doi.org/10.1021/es981162m.

Kratz, S., Schick, J., & Schnug, E. (2016). Trace elements in rock phosphates and P containing mineral and organo-mineral fertilizers sold in Germany. *Science of the Total Environment., 542*, 1013–1019. https://doi.org/10.1016/j.scitotenv.2015.08.046.

Krüger, O., Fiedler, F., Adam, C., Vogel, C., & Senz, R. (2017). Determination of chromium (VI) in primary and secondary fertilizer and their respective precursors. *Chemosphere., 182*, 48–53. https://doi.org/10.1016/j.chemosphere.2017.05.011.

Kumar, M., Kumari, K., Ramanathan, A., & Saxena, R. (2007). A comparative evaluation of groundwater suitability for irrigation and drinking purposes in two intensively cultivated districts of Punjab, India. *Environmental Geology., 53*, 553–574. https://doi.org/10.1007/s00254-007-0672-3.

Kumarathilaka, P., Dissanayake, C. B., & Vithanage, M. (2014). Geochemistry of serpentinite soils: a brief overview. *Journal of Geological Society of Sri Lanka, 16*, 53–63.

Liu, C. W., Lin, K. H., & Kuo, Y. M. (2003). Application of factor analysis in the assessment of groundwater quality in a Blackfoot disease area in Taiwan. *Science of the Total Environment., 313*, 77–89. https://doi.org/10.1016/S0048-9697(02)00683-6.

Manning, A. H., Mills, C. T., Morrison, J. M., & Ball, L. B. (2015). Insights into controls on hexavalent chromium in groundwater provided by environmental tracers, Sacramento Valley, California, USA. *Applied Geochemistry., 62*, 186–199. https://doi.org/10.1016/j.apgeochem.2015.05.010.

Margiotta, S., Mongelli, G., Summa, V., Paternoster, M., & Fiore, S. (2012). Trace element distribution and Cr(VI) speciation in Ca-HCO3 and Mg-HCO3 spring waters from the northern sector of the Pollino massif, southern Italy. *Journal of*

Geochemical Exploration., 115, 1–12. https://doi.org/10.1016/j.gexplo.2012.01.006.

Marques, J. M., Carreira, P. M., Carvalho, M. R., Matias, M. J., Goff, F. E., Basto, M. J., Graça, R. C., Aires-Barros, L., & Rocha, L. (2008). Origins of high pH mineral waters from ultramafic rocks, central Portugal. *Applied Geochemistry., 23*, 3278–3289. https://doi.org/10.1016/j.apgeochem.2008.06.029.

McLay, C. D. A., Dragten, R., Sparling, G., & Selvarajah, N. (2001). Predicting groundwater nitrate concentrations in a region of mixed agricultural land use: a comparison of three approaches. *Environmental Pollution., 115*, 191–204. https://doi.org/10.1016/S0269-7491(01)00111-7.

Megremi, I. (2010a). Distribution and bioavailability of Cr in central Euboea, Greece. *Central European Journal of Geosciences., 2*. https://doi.org/10.2478/v10085-009-0042-3.

Megremi, I. (2010b). *Controlling factors of the mobility and bioavailability of Cr and other metals at the environment of Ni-Laterites*. Ph.D thesis. University of Athens.

Megremi, I., Vasilatos, C., Vassilakis, E., & Economou-Eliopoulos, M. (2019). Spatial diversity of Cr distribution in soil and groundwater sites in relation with land use management in a Mediterranean region: the case of C. Evia and Assopos-Thiva Basins, Greece. *Science of the Total Environment*. https://doi.org/10.1016/j.scitotenv.2018.09.186.

Menció, A., Mas-Pla, J., Otero, N., Regàs, O., Boy-Roura, M., Puig, R., Bach, J., Domènech, C., Zamorano, M., Brusi, D., & Folch, A. (2016). Nitrate pollution of groundwater; all right…, but nothing else? *Science of the Total Environment, The, 539*, 241–251. https://doi.org/10.1016/j.scitotenv.2015.08.151.

Meybeck, M. (1987). Global chemical weathering of surficial rocks estimated from river dissolved loads. *American Journal of Science., 287*, 401–428. https://doi.org/10.2475/ajs.287.5.401.

Mills, C. T., & Goldhaber, M. B. (2012). Laboratory investigations of the effects of nitrification-induced acidification on Cr cycling in vadose zone material partially derived from ultramafic rocks. *Science of the Total Environment., 435-436*, 363–373. https://doi.org/10.1016/j.scitotenv.2012.06.054.

Mills, C. T., Morrison, J. M., Goldhaber, M. B., & Ellefsen, K. J. (2011). Chromium(VI) generation in vadose zone soils and alluvial sediments of the southwestern Sacramento Valley, California: a potential source of geogenic Cr(VI) to groundwater. *Applied Geochemistry, 26*, 1488–1501. https://doi.org/10.1016/j.apgeochem.2011.05.023.

Modaihsh, A., Al-Swailem, M., & Mahjoub, M. (2004). Heavy metals content of commercial inorganic fertilizers used in the Kingdom of Saudi Arabia. *Agricultural and Marine Sciences, 9*, 21–25.

Molina, M., Aburto, F., Calderón, R., Cazanga, M., & Escudey, M. (2009). Trace element composition of selected fertilizers used in Chile: phosphorus fertilizers as a source of long-term soil contamination. *Soil and Sediment Contamination*. https://doi.org/10.1080/15320380902962320.

Moraetis, D., Nikolaidis, N. P., Karatzas, G. P., Dokou, Z., Kalogerakis, N., Winkel, L. H. E., & Palaiogianni-Bellou, A. (2012). Origin and mobility of hexavalent chromium in north-eastern Attica, Greece. *Applied Geochemistry., 27*, 1170–1178. https://doi.org/10.1016/j.apgeochem.2012.03.005.

Morrison, J. M., Goldhaber, M. B., Lee, L., Holloway, J. A. M., Wanty, R. B., Wolf, R. E., & Ranville, J. F. (2009). A regional-scale study of chromium and nickel in soils of northern California, USA. *Applied Geochemistry., 24*, 1500–1511. https://doi.org/10.1016/j.apgeochem.2009.04.027.

Mortvedt, J. J. (1996). Heavy metal contaminants in inorganic and organic fertilizers. *Fertilizer Research., 43*, 55–61. https://doi.org/10.1007/BF00747683.

Nacke, H., Gonçalves, A. C., Schwantes, D., Nava, I. A., Strey, L., & Coelho, G. F. (2013). Availability of heavy metals (Cd, Pb, and Cr) in agriculture from commercial fertilizers. *Archives of Environmental Contamination and Toxicology., 64*, 537–544. https://doi.org/10.1007/s00244-012-9867-z.

Neal, C., & Stanger, G. (1983). Hydrogen generation from mantle source rocks in Oman. *Earth and Planetary Science Letters., 66*, 315–320. https://doi.org/10.1016/0012-821X(83)90144-9.

Nesbit, H. W., & Wilson, R. E. (1992). Recent chemical weathering of basalts. *American Journal of Science., 292*, 740–777. https://doi.org/10.2475/ajs.292.10.740.

Nicholson, F. A., Smith, S. R., Alloway, B. J., Carlton-Smith, C., & Chambers, B. J. (2003). An inventory of heavy metals inputs to agricultural soils in England and Wales. *Science of the Total Environment., 311*, 205–219. https://doi.org/10.1016/S0048-9697(03)00139-6.

Nziguheba, G., & Smolders, E. (2008). Inputs of trace elements in agricultural soils via phosphate fertilizers in European countries. *Science of the Total Environment., 390*, 53–57. https://doi.org/10.1016/j.scitotenv.2007.09.031.

Obiefuna, G., & Orazulike, D. (2011). Physicochemical characteristics of groundwater quality from Yola area, northeastern Nigeria. *Journal of Applied Sciences and Environmental Management., 14*. https://doi.org/10.4314/jasem.v14i1.56468.

OPEKEPE. (2014). *Payment and control agency for guidance and guarantee community aid*. http://www.opekepe.gr/english/. Accessed 15 Feb 2019.

Oze, C., Fendorf, S., Bird, D. K., & Coleman, R. G. (2004). Chromium geochemistry of serpentine soils. *International Geology Review., 46*, 97–126. https://doi.org/10.2747/0020-6814.46.2.97.

Oze, C., Bird, D. K., & Fendorf, S. (2007). Genesis of hexavalent chromium from natural sources in soil and groundwater. *Proceedings of the National Academy of Sciences., 104*, 6544–6549. https://doi.org/10.1073/pnas.0701085104.

Panno, S. V., Kelly, W. R., Martinsek, A. T., & Hackley, K. C. (2006). Estimating background and threshold nitrate concentrations using probability graphs. *Ground Water, 44*, 697–709. https://doi.org/10.1111/j.1745-6584.2006.00240.x.

Papadopoulos, K., & Lappas, I. (2014). Groundwater quality degradation due to Cr6+ presence in Schinos area, prefecture of Corinth, Central Greece. 10th international hydrogeological congress of Greece, Thessaloniki.

Petrilli, F. L., Rossi, G. A., Camoirano, A., Romano, M., Serra, D., Bennicelli, C., de Flora, A., & de Flora, S. (1986). Metabolic reduction of chromium by alveolar macrophages and its relationships to cigarette smoke. *Journal of Clinical*

Investigation., 77, 1917–1924. https://doi.org/10.1172/JCI112520.

Petrotou, A., Skordas, K., Papastergios, G., & Filippidis, A. (2012). Factors affecting the distribution of potentially toxic elements in surface soils around an industrialized area of northwestern Greece. *Environmental Earth Sciences., 65*, 823–833. https://doi.org/10.1007/s12665-011-1127-4.

Piper, A. M. (1944). A graphic procedure in the geochemical interpretation of water-analyses. *Eos, Transactions American Geophysical Union., 25*, 914. https://doi.org/10.1029/TR025i006p00914.

Rajapaksha, A. U., Vithanage, M., Oze, C., Bandara, W. M. A. T., & Weerasooriya, R. (2012). Nickel and manganese release in serpentine soil from the Ussangoda ultramafic complex, Sri Lanka. *Geoderma., 189-190*, 1–9. https://doi.org/10.1016/j.geoderma.2012.04.019.

Rajapaksha, A. U., Vithanage, M., Ok, Y. S., & Oze, C. (2013). Cr(VI) formation related to Cr(III)-muscovite and birnessite interactions in ultramafic environments. *Environmental Science and Technology., 47*, 9722–9729. https://doi.org/10.1021/es4015025.

Rajmohan, N., & Elango, L. (2004). Identification and evolution of hydrogeochemical processes in the groundwater environment in an area of the Palar and Cheyyar River basins, southern India. *Environmental Geology., 1*, 1. https://doi.org/10.1007/s00254-004-1012-5.

Rakhunde, R., Deshpande, L., & Juneja, H. D. (2012). Chemical speciation of chromium in water: a review. *Critical Reviews in Environmental Science and Technology., 42*, 776–810. https://doi.org/10.1080/10643389.2010.534029.

Remoundaki, E., Vasileiou, E., Philippou, A., Perraki, M., Kousi, P., Hatzikioseyian, A., & Stamatis, G. (2016). Groundwater deterioration: the simultaneous effects of intense agricultural activity and heavy metals in soil. *Procedia Engineering*. https://doi.org/10.1016/j.proeng.2016.11.099.

Richard, F. C., & Bourg, A. C. M. (1991). Aqueous geochemistry of chromium: a review. *Water Research, 25*, 807–816. https://doi.org/10.1016/0043-1354(91)90160-R.

Robles-Camacho, J., & Armienta, M. (2000). Natural chromium contamination of groundwater at León Valley, México. *Journal of Geochemical Exploration., 68*, 167–181. https://doi.org/10.1016/S0375-6742(99)00083-7.

Rose, S. (2002). Comparative major ion geochemistry of Piedmont streams in the Atlanta, Georgia region: possible effects of urbanization. *Environmental Geology., 42*, 102–113. https://doi.org/10.1007/s00254-002-0545-8.

Ryan, P. C., Kim, J., Wall, A. J., Moen, J. C., Corenthal, L. G., & Chow, D. R. (2011). Ultramafic-derived arsenic in a fractured bedrock aquifer. *Applied Geochemistry, 26*, 444–457. https://doi.org/10.1016/j.apgeochem.2011.01.004.

Sager, M. (1997). Possible trace metal load from fertilizers. *Die Bodenkultur, 48*, 217–223.

Saha, R., Nandi, R., & Saha, B. (2011). Sources and toxicity of hexavalent chromium. *Journal of Coordination Chemistry., 64*, 1782–1806. https://doi.org/10.1080/00958972.2011.583646.

Schoeller, H. (1977). *Geochemistry of groundwater. In: Groundwater studies: an international guide for research and practice* (pp. 1–18). Paris: UNESCO.

Singh, A. K., Raj, B., Tiwari, A. K., & Mahato, M. K. (2013). Evaluation of hydrogeochemical processes and groundwater quality in the Jhansi district of Bundelkhand region, India. *Environmental Earth Sciences., 70*, 1225–1247. https://doi.org/10.1007/s12665-012-2209-7.

Singh, N., Singh, R. P., Kamal, V., Sen, R., & Mukherjee, S. (2014). Assessment of hydrogeochemistry and the quality of groundwater in 24-Parganas districts, West Bengal. *Environmental Earth Sciences., 73*, 375–386. https://doi.org/10.1007/s12665-014-3431-2.

Smith, K. S., & Huyck, H. L. O. (1999). An overview of the abundance, relative mobility, bioavailability and human toxicity of metals. In G. S. Plumlee & M. J. Logsdon (Eds.), *The environmental geochemistry of mineral deposits. Part A: processes, techniques and health issues* (pp. 29–70). Littleton: Society of Economic Geologists.

Stamatis, G., Alexakis, D., Gamvroula, D., & Migiros, G. (2011). Groundwater quality assessment in Oropos-Kalamos basin, Attica, Greece. *Environmental Earth Sciences., 64*, 973–988. https://doi.org/10.1007/s12665-011-0914-2.

Subramani, T., Rajmohan, N., & Elango, L. (2010). Groundwater geochemistry and identification of hydrogeochemical processes in a hard rock region, southern India. *Environmental Monitoring and Assessment., 162*, 123–137. https://doi.org/10.1007/s10661-009-0781-4.

Tashakor, M., Modabberi, S., van der Ent, A., & Echevarria, G. (2018). Impacts of ultramafic outcrops in Peninsular Malaysia and Sabah on soil and water quality. *Environmental Monitoring and Assessment., 190*, 333. https://doi.org/10.1007/s10661-018-6668-5.

Toumi, N., Hussein, B. H. M., Rafrafi, S., & El kassas, N. (2015). Groundwater quality and hydrochemical properties of Al-Ula region, Saudi Arabia. *Environmental Monitoring and Assessment., 187*. https://doi.org/10.1007/s10661-014-4241-4.

Tsioumas, B., & Zorapas, B. (2004). *Causes of groundwater salinisation in the western part of the Psachna plain in Evia*. Athens: Institute of Geological and Mining Exploration (in Greek).

Tziritis, E., Kelepertzis, E., Korres, G., Perivolaris, D., & Repani, S. (2012). Hexavalent chromium contamination in groundwaters of Thiva Basin, central Greece. *Bulletin of Environmental Contamination and Toxicology., 89*, 1073–1077. https://doi.org/10.1007/s00128-012-0831-4.

Tziritis, E., Skordas, K., & Kelepertzis, A. (2016). The use of hydrogeochemical analyses and multivariate statistics for the characterization of groundwater resources in a complex aquifer system. A case study in Amyros River basin, Thessaly, central Greece. *Environmental Earth Sciences, 75*. https://doi.org/10.1007/s12665-015-5204-y.

USEPA. (2011). *Chromium in drinking water*. United States Environmental Protection Agency. https://www.epa.gov/dwstandardsregulations/chromium-drinking-water. Accessed 15 Feb 2019.

USEPA. (2014). *Toxic and priority pollutants under the clean water act*. Available at: https://www.epa.gov/eg/toxic-and-priority-pollutants-under-clean-water-act#priority. Accessed 15 Feb 2019.

Vasileiou, E., Perraki, M., Stamatis, G., & Gartzos, E. (2014a). Hydrochemical characteristics of groundwater in central Euboea. 10th international hydrogeological congress of Greece, Thessaloniki, 2014 (in Greek).

Vasileiou, E., Perraki, M., Stamatis, G., & Gartzos, E. (2014b). The effects of water rock interaction and the human activities on the occurrence of hexavalent chromium in waters. The case study of the Psachna basin, central Euboea, Greece. EGU General Assembly 2014, 27 April–2 May, 2014 in Vienna, Austria, id.15467.

Voutsis, N., Kelepertzis, E., Tziritis, E., & Kelepertzis, A. (2015). Assessing the hydrogeochemistry of groundwaters in ophiolite areas of Euboea Island, Greece, using multivariate statistical methods. *Journal of Geochemical Exploration., 159*, 79–92. https://doi.org/10.1016/j.gexplo.2015.08.007.

VROM. (2000). Circular on target values and intervention values for soil remediation. Netherlands Government Gazette.

Ward, J. H. (1963). Hierarchical grouping to optimize an objective function. *Journal of the American Statistical Association, 58*.

Weng, T. N., Liu, C. W., Kao, Y. H., & Hsiao, S. S. Y. (2017). Isotopic evidence of nitrogen sources and nitrogen transformation in arsenic-contaminated groundwater. *Science of the Total Environment., 578*, 167–185. https://doi.org/10.1016/j.scitotenv.2016.11.013.

Wilbur, S., Ingerman, L., Citra, M., Osier, M., & Wohlers, D. (2000). *Toxicological profile for chromium*. Atlanta: Agency for Toxic Substances and Disease Registry. http://www.atsdr.cdc.gov/toxprofiles/tp7.pdf. Accessed 15 Feb 2019.

World Health Organization (WHO). (2011). *Guidelines for drinking water quality* (4th ed.). Geneva: World Health Organization.

Zaidi, F. K., Nazzal, Y., Jafri, M. K., Naeem, M., & Ahmed, I. (2015). Reverse ion exchange as a major process controlling the groundwater chemistry in an arid environment: a case study from northwestern Saudi Arabia. *Environmental Monitoring and Assessment., 187*. https://doi.org/10.1007/s10661-015-4828-4.

Zhang, J., Huang, W. W., Létolle, R., & Jusserand, C. (1995). Major element chemistry of the Huanghe (Yellow River), China—weathering processes and chemical fluxes. *Journal of Hydrology., 168*, 173–203. https://doi.org/10.1016/0022-1694(94)02635-O.

Zhang, W., Singh, P., Paling, E., & Delides, S. (2004). Arsenic removal from contaminated water by natural iron ores. *Minerals Engineering, 17*, 517–524. https://doi.org/10.1016/j.mineng.2003.11.020.

Zhang, Y., Li, F., Zhang, Q., Li, J., & Liu, Q. (2014). Tracing nitrate pollution sources and transformation in surface- and ground-waters using environmental isotopes. *Science of the Total Environment., 490*, 213–222. https://doi.org/10.1016/j.scitotenv.2014.05.004.

Zhitkovich, A. (2011). Chromium in drinking water: Sources, metabolism, and cancer risks. *Chemical Research in Toxicology., 24*, 1617–1629. https://doi.org/10.1021/tx200251t.